NASA TECHNICAL NOTE

NASA TN D-7973

NASA TN D-7973

SECOND-ORDER SMALL-DISTURBANCE SOLUTIONS FOR HYPERSONIC FLOW OVER POWER-LAW BODIES

James C. Townsend

Langley Research Center
Hampton, Va. 23665

NATIONAL AERONAUTICS AND SPACE ADMINISTRATION • WASHINGTON, D. C. • NOVEMBER 1975

1. Report No.	2. Government Accession No.	3. Recipient's Catalog No.
NASA TN D-7973		

4. Title and Subtitle

SECOND-ORDER SMALL-DISTURBANCE SOLUTIONS FOR HYPERSONIC FLOW OVER POWER-LAW BODIES

5. Report Date: November 1975

6. Performing Organization Code:

7. Author(s): James C. Townsend

8. Performing Organization Report No.: L-10154

9. Performing Organization Name and Address:
NASA Langley Research Center
Hampton, Va. 23665

10. Work Unit No.: 505-11-15-02

11. Contract or Grant No.:

12. Sponsoring Agency Name and Address:
National Aeronautics and Space Administration
Washington, D.C. 20546

13. Type of Report and Period Covered: Technical Note

14. Sponsoring Agency Code:

15. Supplementary Notes:

16. Abstract

Similarity solutions have been found which give the adiabatic flow of an ideal gas about two-dimensional and axisymmetric power-law bodies at infinite Mach number to second order in the body slenderness parameter. The flow variables were expressed as a sum of zero-order and perturbation similarity functions for which the axial variations in the flow equations separated out. The resulting similarity equations were integrated numerically. The solutions, which are universal functions, are presented in graphic and tabular form. To avoid a singularity in the calculations, the results are limited to body power-law exponents greater than about 0.85 for the two-dimensional case and 0.75 for the axisymmetric case. Because of the entropy layer induced by the nose bluntness (for power-law bodies other than cones and wedges), only the pressure function is valid at the body surface.

The similarity results give excellent agreement with the exact solutions for inviscid flow over wedges and cones having half-angles up to about 20°. They give good agreement with experimental shock-wave shapes and surface-pressure distributions for 3/4-power axisymmetric bodies, considering that Mach number and boundary-layer displacement effects are not included in the theory.

17. Key Words (Suggested by Author(s))
Hypersonic flow
Power-law body
Hypersonic similarity
Perturbation method
Second-order solutions

18. Distribution Statement
Unclassified – Unlimited

Subject Category 02

19. Security Classif. (of this report)	20. Security Classif. (of this page)	21. No. of Pages	22. Price*
Unclassified	Unclassified	65	$4.25

*For sale by the National Technical Information Service, Springfield, Virginia 22161

CONTENTS

SECOND-ORDER SMALL-DISTURBANCE SOLUTIONS FOR HYPERSONIC FLOW OVER POWER-LAW BODIES

James C. Townsend
Langley Research Center

SUMMARY

Similarity solutions have been found which give the adiabatic flow of an ideal gas about two-dimensional and axisymmetric power-law bodies at infinite Mach number to order-δ^2, where δ is a body slenderness parameter. These solutions were obtained by a perturbation method wherein the flow variables are expressed as series of similarity functions and the axial variations in the flow equations separate out. The resulting similarity equations were numerically integrated from the shock wave, where the boundary conditions are known from the Rankine-Hugoniot relations, toward the body. The order-δ^2 solutions are limited to body power-law exponents greater than 0.85 for two-dimensional flow and 0.75 for axisymmetric flow to avoid a singularity in the shock-displacement calculation. The solutions, which are independent of the slenderness parameter δ and, thus, are universal functions, are presented in tabular and graphic form. Because of the entropy layer induced by the nose bluntness (for power-law bodies other than cones or wedges) the velocity and density functions are not valid at the body surface, but the pressure function is unaffected.

In comparisons with the exact solutions for inviscid flow over wedges and cones, the order-δ^2 similarity results give excellent agreement for δ values up to 0.4, corresponding to wedge or cone angles up to about 20°. In comparisons with experimental shock-wave shapes and surface-pressure distributions for 3/4-power axisymmetric bodies, the order-δ^2 similarity solutions give good results, considering that Mach number and boundary-layer displacement effects are not included in the theory. For body fineness ratios near 2, the effects of the order-δ^2 terms are significant only very near the body nose, whereas for a fineness ratio near 1 the order-δ^2 terms have a large effect over almost the entire body.

Although the order-δ^2 similarity solutions are developed for infinite Mach number, the derivation shows that they are compatible with shock-strength perturbation solutions, which introduce Mach number effects.

INTRODUCTION

A great deal of research has gone into finding solutions to the hypersonic small-disturbance form of the inviscid adiabatic-flow equations. One area that has received particular attention is that of similarity solutions for power-law profile bodies. (See refs. 1 to 6.) Since these studies have all begun with the small-disturbance equations, obtained by neglecting terms containing the body thickness ratio, their solutions also neglect the effects of body thickness. The purpose of the present study was to obtain second-order similarity solutions for power-law bodies by retaining all second-order terms in the body-thickness ratio. (As will be seen, there are no first-order terms in the body thickness and, thus, no first-order solutions in the thickness parameter.)

The similarity solutions referred to herein are solutions for self-similar flows, that is, flows for which the flow field between the shock wave and the body can be expressed in terms of functions which (in suitable coordinates) are independent of one of the coordinate directions. Inviscid axisymmetric supersonic flow over a cone with an attached shock wave is a classical example of a self-similar flow and represents a particular case of the similar solutions discussed herein. For the cone, the flow-field properties (e.g., the pressure, the density, and the velocity components) are themselves constant along rays from the cone vertex. For the other power-law bodies, the flow-field properties are not constant themselves, but similarity functions describing these properties are constant (to the order of the solution) along curved power-law paths from the nose of the body. The similar-solution approach to solving the flow equations is valuable because it allows a reduction in the number of independent variables in the problem. In particular, for hypersonic flow about power-law bodies, the similarity approach reduces a system of partial differential equations to a system of ordinary differential equations.

Kubota (ref. 3) obtained numerical solutions for the self-similar flow fields about bodies having power-law profiles in the limits of infinite Mach number and very slender bodies (the "zero-order" case). He also applied a perturbation in a shock strength parameter and numerically obtained first-order similar solutions for moderately strong shock waves. Mirels (ref. 4) computed additional and more accurate numerical results for the zero-order and moderately strong shock-wave cases. He also derived approximate analytical solutions for these cases. Hayes and Probstein (ref. 5) described the general development of similarity solutions and emphasized the contributions of foreign authors. Mirels (ref. 6) treated all of the important developments in the use of hypersonic small-disturbance theory to obtain solutions for power-law bodies in a unified way, and added an analysis of perturbed power-law body shapes.

Only a few experimental investigations of the flow field over power-law bodies have been made. Kubota (ref. 3) compared his theoretical results to measurements of

surface-pressure distributions and shock-wave shapes for 2/3- and 3/4-power bodies and obtained good agreement for the more slender bodies. Peckham (ref. 7) measured pressure distributions and shock-wave shapes for a series of power-law bodies, some of which fall in the similar-solution range. Freeman, Cash, and Bedder (ref. 8) and Beavers (ref. 9) also presented detailed shock-shape data for a series of power-law bodies and registered some disagreement with Kubota's results. Spencer and Fox (ref. 10) presented aerodynamic drag and other data for several power-law bodies over a wide Mach number range. Ashby (ref. 11) presented aerodynamic data for a similar series of bodies over a range of Reynolds numbers at a Mach number of 6, and Ashby and Harris (ref. 12) used a method of characteristics and boundary-layer computer programs to show the important effect of boundary-layer transition on the total drag of those bodies.

Townsend (ref. 13) applied the zero-order solution of Kubota and Mirels, with their shock-strength parameter perturbation and with a boundary-layer displacement correction, to the problem of estimating the forces and moments on a half-axisymmetric body under a thin, flat wing. In order to study a range of configurations at a moderately hypersonic Mach number, Townsend applied his method to configurations which are marginally slender (i.e., to configurations for which the errors arising from body thickness are small but not negligible). This type of application points up two reasons for seeking solutions which include the effects of the second-order terms for body slenderness in the flow equations: (1) to assess the error caused by making the small-disturbance assumption, and (2) to improve the accuracy of calculations for marginally slender bodies.

In the present study the second-order similarity solutions were obtained by a perturbation method. This method used expansions of the variables in terms of the body slenderness parameter to obtain higher order solutions as perturbations from the known zero-order solution. This approach is very similar to that of Kubota and Mirels in obtaining their first-order solutions in terms of a small strong-shock parameter. A more detailed presentation of the theoretical development is given in reference 14.

SYMBOLS

a_1, a_2 shock-wave displacement constants (eq. (6))

C_p pressure coefficient, $\dfrac{\bar{p} - \bar{p}_\infty}{\bar{q}_\infty}$

$\bar{D}$ length constant in shock-shape correlation (fig. 11)

f	body fineness ratio, $\frac{\text{Length}}{\text{Maximum thickness}}$
F	similarity pressure function
$\bar{l}$	body length
m	power-law exponent
M_∞	free-stream Mach number
p	pressure
$\bar{q}_\infty$	free-stream dynamic pressure, $\frac{1}{2}\bar{\rho}_\infty \bar{u}_\infty^2$
r	lateral coordinate
R	lateral coordinate of shock wave
T	temperature
u	longitudinal-velocity perturbation
$\bar{u}_\infty$	free-stream velocity
v	lateral velocity
V	velocity
x	longitudinal coordinate
β	alternate shock-shape parameter, $\frac{2(1 - m)}{(1 + \sigma)m}$
γ	ratio of specific heats
δ	body slenderness parameter, $\frac{R_0(\bar{l})}{\bar{l}}$
ϵ	shock-wave strength parameter, $(\delta M_\infty)^{-2}$

η	similarity lateral coordinate
θ_b	body surface angle
θ_s	shock-wave angle
θ_0	similarity stream function
ν	similarity longitudinal-velocity function
ξ	similarity longitudinal coordinate
ρ	density
σ	constant with value 0 for planar flow and 1 for axisymmetric flow
ϕ	similarity lateral-velocity function
ψ	similarity density function

Subscripts:

a	part of decomposed function multiplied by a_2 (eqs. (22))
b	body surface
c	part of decomposed function independent of a_2 (eqs. (22))
s	shock wave
t	total
0	zero order
1	order-ϵ
2	order-δ^2
∞	free stream

A prime denotes the derivative of a function of one variable. A bar over a variable denotes that it has physical dimensions. Normalized variables (without a bar) are given in equations (1).

THEORY

Transformation of Basic Flow Equations

Normalization.- The initial treatment of the basic flow equations follows that of Kubota (ref. 3) (also covered by Mirels in ref. 6), except that no terms are dropped. They showed that for slender bodies in hypersonic flow the variables can be normalized by using the expressions

$$\left.\begin{aligned} x &= \frac{\bar{x}}{\bar{l}} & r &= \frac{\bar{r}}{\delta \bar{l}} & p &= \frac{\bar{p}}{\delta^2 \bar{\rho}_\infty \bar{u}_\infty^2} \\ \rho &= \frac{\bar{\rho}}{\bar{\rho}_\infty} & u &= \frac{\bar{u} - \bar{u}_\infty}{\delta^2 \bar{u}_\infty} & v &= \frac{\bar{v}}{\delta \bar{u}_\infty} \end{aligned}\right\} \tag{1}$$

The symbol δ is a body slenderness parameter (to be discussed later) introduced so as to make the dimensionless variables of order unity. These variables are substituted into the complete inviscid adiabatic-flow equations to obtain the following normalized flow equations:

Continuity:

$$\delta^2 \frac{\partial \rho u}{\partial x} + \frac{\partial \rho}{\partial x} + \frac{\partial \rho v}{\partial r} + \sigma \frac{\rho v}{r} = 0$$

Longitudinal momentum:

$$\delta^2 u \frac{\partial u}{\partial x} + \frac{\partial u}{\partial x} + v \frac{\partial u}{\partial r} + \frac{1}{\rho} \frac{\partial p}{\partial x} = 0$$

Lateral momentum:

$$\delta^2 u \frac{\partial v}{\partial x} + \frac{\partial v}{\partial x} + v \frac{\partial v}{\partial r} + \frac{1}{\rho} \frac{\partial p}{\partial r} = 0$$

Energy:

$$\left(\delta^2 u \frac{\partial}{\partial x} + \frac{\partial}{\partial x} + v \frac{\partial}{\partial r}\right)\left(\frac{p}{\rho^\gamma}\right) = 0$$

(2)

The constant σ in the continuity equation has the value 0 for planar flow (Cartesian coordinates) or the value 1 for axisymmetric flow (cylindrical coordinates). Note that each of these equations contains a leading term in δ^2. If the body were sufficiently slender, the order-δ^2 terms could be dropped, thus leaving the hypersonic small-disturbance equations used by other workers. For the present study, however, the equations are retained in the complete form.

Similarity variables.- The next step is to put the flow variables into similarity forms. Following Kubota's method, these forms will be selected so as to agree with the flow through the oblique bow shock wave. The normalized flow variables just behind an oblique shock are (ref. 15)

$$\left.\begin{aligned} p_s &= \frac{1}{\gamma\delta^2 M_\infty{}^2}\,\frac{2\gamma M_\infty{}^2 \sin^2\theta_s - (\gamma - 1)}{\gamma + 1} \\ \rho_s &= \frac{(\gamma + 1)M_\infty{}^2 \sin^2\theta_s}{(\gamma - 1)M_\infty{}^2 \sin^2\theta_s + 2} \\ u_s &= \frac{1}{\delta^2}\left[\frac{-2\left(M_\infty{}^2 \sin^2\theta_s - 1\right)}{(\gamma + 1)M_\infty{}^2}\right] \\ v_s &= \frac{1}{\delta}\left[\frac{2\left(M_\infty{}^2 \sin^2\theta_s - 1\right)}{(\gamma + 1)M_\infty{}^2}\right]\cot\theta_s \end{aligned}\right\} \tag{3}$$

If the shock-wave shape is given by $R(x)$, its slope is $\bar{R}'(\bar{x}) \equiv \frac{d\bar{R}}{d\bar{x}} = \delta\frac{dR}{dx} = \delta R'$. The shock-wave angle θ_s is related to the slope by $\tan\theta_s = \delta R'$, from which $\sin^2\theta_s = \frac{\delta^2 R'^2}{1 + \delta^2 R'^2}$. Putting these results into the oblique-shock relations gives the pressure (for R' of order unity):

$$\begin{aligned} p_s &= \frac{2}{\gamma + 1}\left[\frac{R'^2}{1 + \delta^2 R'^2} - \frac{\gamma - 1}{2\gamma}\epsilon\right] \\ &= \frac{2}{\gamma + 1}R'^2 - \frac{2}{\gamma + 1}\delta^2 R'^4 - \frac{\gamma - 1}{\gamma + 1}\frac{\epsilon}{\gamma} + O(\delta^4) \end{aligned} \tag{4a}$$

Similarly, the other flow variables at the shock are

$$\rho_s = \frac{\gamma + 1}{\gamma - 1} - \frac{2(\gamma + 1)}{(\gamma - 1)^2} \frac{\epsilon}{R'^2} + O(\delta^4) \tag{4b}$$

$$u_s = -\frac{2}{\gamma + 1} R'^2 + \frac{2}{\gamma + 1} \delta^2 R'^4 + \frac{2}{\gamma + 1} \epsilon + O(\delta^4) \tag{4c}$$

$$v_s = \frac{2}{\gamma + 1} R' - \frac{2}{\gamma + 1} \delta^2 R'^3 - \frac{2}{\gamma + 1} \frac{\epsilon}{R'} + O(\delta^4) \tag{4d}$$

where $\epsilon \equiv \frac{1}{\delta^2 M_\infty^2}$ is a shock-strength parameter; and as $\epsilon \to 0$, $\frac{\bar{\rho}_s}{\bar{\rho}_\infty} \to \frac{\gamma + 1}{\gamma - 1}$, the limiting value for shock-wave strength.

At this point, in order to get an expression for the shock-wave shape, consideration is narrowed to flows about power-law bodies. Under the hypersonic small-disturbance assumptions, a power-law body $\left(r_b \sim x^m\right)$ produces a power-law shock wave $\left(R \sim x^m\right)$ for $\frac{2}{3 + \sigma} < m \leqq 1$. (See ref. 2.) Specifically, for $\delta^2 \to 0$ and $\epsilon \to 0$, a body $r_b = \frac{1}{2\delta f} x^m$ produces the zero-order shock shape $R_0 = x^m$. (See figs. 1(a) and 1(b).) Note that for $m = 1$ the body is a wedge (for $\sigma = 0$) or a cone (for $\sigma = 1$), both of which are known to have straight shock waves and therefore satisfy the aforementioned relations.

The expression for the zero-order shock-wave shape serves to define the slenderness parameter δ. That is, $\bar{R}_0(\bar{x}) = \delta \bar{l} \left(\frac{\bar{x}}{\bar{l}}\right)^m$ evaluated at $\bar{x} = \bar{l}$ gives the relation $\delta = \frac{\bar{R}_0(\bar{l})}{\bar{l}}$. Thus, δ is the tangent of an angle defined by the shock-wave position (fig. 1(a)) and is, in fact, a "mean shock-wave angle" parameter. However, the shock lies near the body so that the shock-wave angle and body slenderness are closely related.

To aid in the separation of variables, a shock-oriented coordinate system is now introduced (fig. 1(c)). This system has

$$\xi = x \qquad \eta = \frac{r}{R_0} \tag{5}$$

so that $r = \eta R_0 = \eta x^m = \eta \xi^m$. The body surface is then $r_b = \eta_b \xi^m$, where $\eta_b = \frac{1}{2\delta f}$.

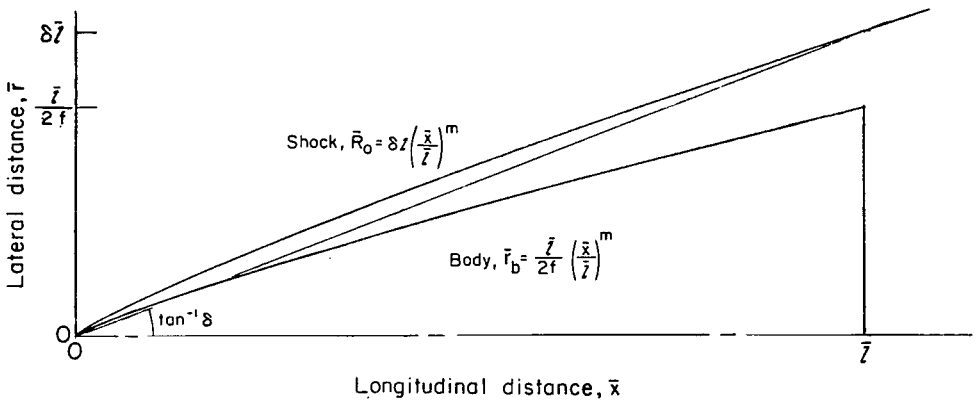

(a) Physical coordinate system (shown with $\delta = 0.4$).

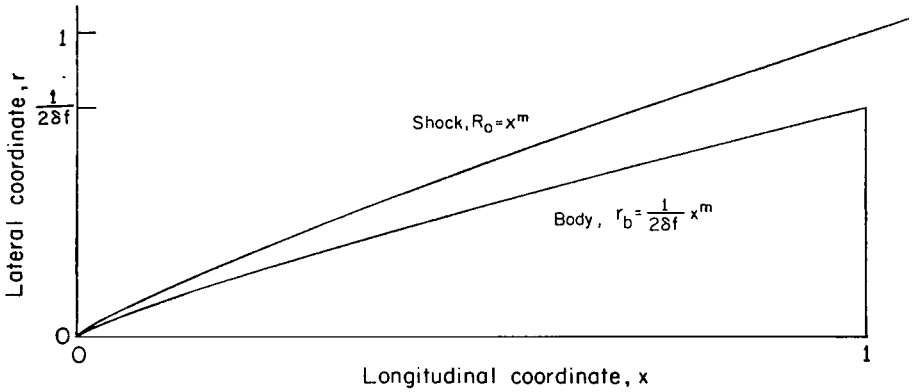

(b) Normalized coordinate system.

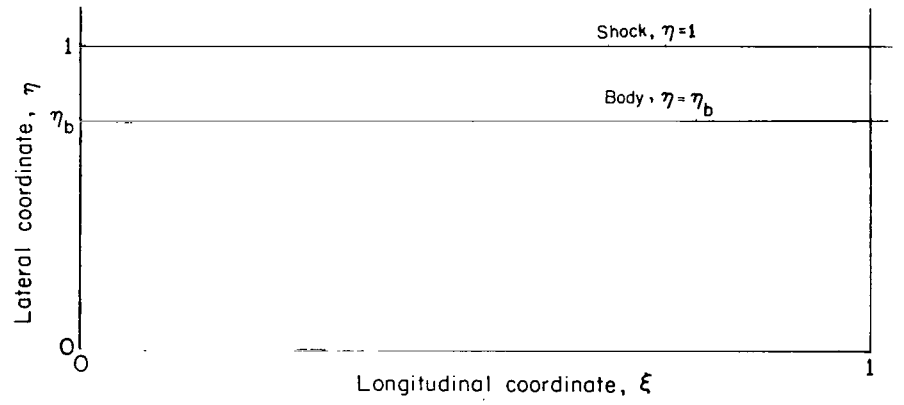

(c) Similarity coordinate system.

Figure 1.- Power-law body and zero-order shock in physical and transformed coordinate systems (shown with $m = 0.85$ and $\sigma = 0$).

The shock-wave shape to be used in equations (4) is the zero-order shock with Kubota's shock-strength perturbation (ref. 3) and a separate perturbation for the body slenderness. It is taken to be

$$R(\xi) = \xi^{m}\left[1 + \delta^{2}a_{2}m^{2}\xi^{-2(1-m)} + \epsilon a_{1}\xi^{2(1-m)}\right] \tag{6}$$

where the exponents are of the form required for similarity and the constants a_1 and a_2 are to be determined as part of the solution.

Substituting the shock-wave slope (derivative of eq. (6)) into the expanded oblique-shock relations (eqs. (4)) and ordering the terms by powers of δ and ϵ suggest expressions for the flow variables in the following form (neglecting terms of order δ^4 and of order ϵ^2):

$$\left.\begin{aligned} p(\xi,\eta) &= F_0(\eta)m^2\xi^{-2(1-m)} + \epsilon F_1(\eta)m^2 + \delta^2 F_2(\eta)m^4\xi^{-4(1-m)} \\ \rho(\xi,\eta) &= \psi_0(\eta) + \epsilon\psi_1(\eta)\xi^{2(1-m)} + \delta^2\psi_2(\eta)m^2\xi^{-2(1-m)} \\ u(\xi,\eta) &= \nu_0(\eta)m^2\xi^{-2(1-m)} + \epsilon\nu_1(\eta)m^2 + \delta^2\nu_2(\eta)m^4\xi^{-4(1-m)} \\ v(\xi,\eta) &= \phi_0(\eta)m\xi^{-(1-m)} + \epsilon\phi_1(\eta)\xi^{(1-m)} + \delta^2\phi_2(\eta)m^3\xi^{-3(1-m)} \end{aligned}\right\} \tag{7}$$

Here, functions of $\eta = r/R_0$ replace the constant coefficients of the shock relations.

Transformed flow equations.- Equations (7) are substituted into the normalized flow equations (2), noting that

$$\left.\begin{aligned} \frac{\partial}{\partial x} &= \frac{\partial\xi}{\partial x}\frac{\partial}{\partial\xi} + \frac{\partial\eta}{\partial x}\frac{\partial}{\partial\eta} = \frac{\partial}{\partial\xi} - \frac{m\eta}{\xi}\frac{\partial}{\partial\eta} \\ \frac{\partial}{\partial r} &= \frac{\partial\xi}{\partial r}\frac{\partial}{\partial\xi} + \frac{\partial\eta}{\partial r}\frac{\partial}{\partial\eta} = \frac{1}{\xi^{m}}\frac{\partial}{\partial\eta} \end{aligned}\right\} \tag{8}$$

Then, the flow equations (2) become (away from the nose $\xi = 0$):

Continuity:

$$\left[\psi_0\left(\phi_0' + \frac{\sigma}{\eta}\,\phi_0\right) - (\eta - \phi_0)\,\psi_0'\right] m\xi^{-1} + \epsilon\left\{\psi_0\phi_1' + \left(\psi_0' + \frac{\sigma}{\eta}\,\psi_0\right)\phi_1\right.$$

$$\left. + \left[\phi_0' + \frac{\sigma}{\eta}\,\phi_0 + 2\left(\frac{1-m}{m}\right)\right]\psi_1 - (\eta - \phi_0)\,\psi_1'\right\}\frac{1}{m}\,\xi^{1-2m}$$

$$+ \delta^2\left\{\psi_0\phi_2' + \left(\psi_0' + \frac{\sigma}{\eta}\,\psi_0\right)\phi_2 + \left[\phi_0' + \frac{\sigma}{\eta}\,\phi_0 - 2\left(\frac{1-m}{m}\right)\right]\psi_2 - (\eta - \phi_0)\,\psi_2'\right.$$

$$\left. - \eta\nu_0\psi_0' - \left[\eta\nu_0' + 2\left(\frac{1-m}{m}\right)\nu_0\right]\psi_0\right\} m^3\xi^{-3+2m} + O(\delta^4) = 0 \qquad (9a)$$

Longitudinal momentum:

$$\left[(\eta - \phi_0)\,\nu_0' + \eta\,\frac{F_0'}{\psi_0} + 2\left(\frac{1-m}{m}\right)\left(\nu_0 + \frac{F_0}{\psi_0}\right)\right] m^3\xi^{-3+2m}$$

$$+ \epsilon\left\{(\eta - \phi_0)\,\nu_1' + \eta\,\frac{F_1'}{\psi_0} - \frac{1}{\psi_0^2}\left[\eta F_0' + 2\left(\frac{1-m}{m}\right)F_0\right]\psi_1 - \nu_0'\phi_1\right\} m^3\xi^{-1}$$

$$+ \delta^2\left\{(\eta - \phi_0)\,\nu_2' + \eta\,\frac{F_2'}{\psi_0} + 4\left(\frac{1-m}{m}\right)\left(\nu_2 + \frac{F_2}{\psi_0}\right) - \nu_0'\phi_2 - \frac{1}{\psi_0^2}\left[\eta F_0' + 2\left(\frac{1-m}{m}\right)F_0\right]\psi_2\right.$$

$$\left. + \nu_0\left[\eta\nu_0' + 2\left(\frac{1-m}{m}\right)\nu_0\right]\right\} m^5\xi^{-5+4m} + O(\delta^4) = 0 \qquad (9b)$$

Lateral momentum:

$$\left[(\eta - \phi_0)\phi_0' - \frac{F_0'}{\psi_0} + \left(\frac{1-m}{m}\right)\phi_0\right] m^2 \xi^{-2+m} + \epsilon\left\{(\eta - \phi_0)\phi_1' - \frac{F_1'}{\psi_0} + \frac{F_0'}{\psi_0^2}\psi_1\right.$$

$$\left. - \left[\phi_0' + \left(\frac{1-m}{m}\right)\right]\phi_1\right\} m^2 \xi^{-m} + \delta^2\left\{(\eta - \phi_0)\phi_2' - \frac{F_2'}{\psi_0} + \frac{F_0'}{\psi_0^2}\psi_2\right.$$

$$\left. - \left[\phi_0' - 3\left(\frac{1-m}{m}\right)\right]\phi_2 + \left[\eta\phi_0' + \left(\frac{1-m}{m}\right)\phi_0\right]\nu_0\right\} m^4 \xi^{-4+3m} + O(\delta^4) = 0 \qquad (9c)$$

Energy:

$$\left[(\eta - \psi_0)\left(\gamma\frac{\psi_0'}{\psi_0} - \frac{F_0'}{F_0}\right) - 2\left(\frac{1-m}{m}\right)\right] m\xi^{-1} + \epsilon\left\{(\eta - \phi_0)\left[\left(\gamma\frac{\psi_1'}{\psi_0} - \frac{F_1'}{F_0}\right)\right.\right.$$

$$\left.\left. - \left(\gamma\frac{\psi_1\psi_0'}{\psi_0^2} - \frac{F_1F_0'}{F_0^2}\right)\right] - 2\left(\frac{1-m}{m}\right)\left(\gamma\frac{\psi_1}{\psi_0} - \frac{F_1}{F_0}\right) - \left(\gamma\frac{\psi_0'}{\psi_0} - \frac{F_0'}{F_0}\right)\phi_1\right\} m\xi^{1-2m}$$

$$+ \delta^2\left\{(\eta - \phi_0)\left[\left(\gamma\frac{\psi_2'}{\psi_0} - \frac{F_2'}{F_0}\right) - \left(\gamma\frac{\psi_2\psi_0'}{\psi_0^2} - \frac{F_2F_0'}{F_0^2}\right)\right] + 2\left(\frac{1-m}{m}\right)\left(\gamma\frac{\psi_2}{\psi_0} - \frac{F_2}{F_0}\right)\right.$$

$$\left. - \left(\gamma\frac{\psi_0'}{\psi_0} - \frac{F_0'}{F_0}\right)\phi_2 - \left[2\left(\frac{1-m}{m}\right) - \eta\left(\gamma\frac{\psi_0'}{\psi_0} - \frac{F_0'}{F_0}\right)\right]\nu_0\right\} m^3\xi^{-3+2m} + O(\delta^4) = 0 \qquad (9d)$$

These are ordinary first-order differential equations that are linear in the derivatives of the functions defining the pressure, density, and velocity fields. It is noteworthy that although δ appears to the first power in the normalization of variables (eqs. (1)), only the even powers of δ appear in the final form of the flow equations. Thus, although the solutions to be found are of second order in the body slenderness parameter δ, they could be considered of first order in δ^2. To avoid any ambiguity they will generally be referred to as order-δ^2 solutions.

Similarity equations.- Since the general similarity solutions being sought do not depend on the particular values of δ or ϵ, each of the three major terms in each of the four conservation equations (9) must be separately equal to zero. Therefore, the terms can be separated into 12 equations in the 12 unknown functions F_0, ψ_0, ν_0, ϕ_0, F_1, ψ_1, ν_1, ϕ_1, F_2, ψ_2, ν_2, and ϕ_2. Eight of these equations form the zero-order and order-ϵ systems of equations found by Kubota (ref. 3).

The zero-order equations are as follows:

Continuity:

$$\psi_0\left(\phi_0' + \frac{\sigma}{\eta}\phi_0\right) - (\eta - \phi_0)\psi_0' = 0$$

Longitudinal momentum:

$$(\eta - \phi_0)\nu_0' + \eta\frac{F_0'}{\psi_0} + 2\left(\frac{1 - m}{m}\right)\left(\nu_0 + \frac{F_0}{\psi_0}\right) = 0$$

Lateral momentum:

$$(\eta - \phi_0)\phi_0' - \frac{F_0'}{\psi_0} + \left(\frac{1 - m}{m}\right)\phi_0 = 0$$

Energy:

$$(\eta - \phi_0)\left(\gamma\frac{\psi_0'}{\psi_0} - \frac{F_0'}{F_0}\right) - 2\left(\frac{1 - m}{m}\right) = 0$$

(10)

These equations are the same as the case first studied by Kubota, except that he omitted the longitudinal-momentum equation, which is uncoupled from the others. These equations contain only one parameter, the power-law exponent m. Thus, for two-dimensional flow ($\sigma = 0$) or axisymmetric flow ($\sigma = 1$) of a given gas, the similar solutions $F_0(\eta)$, $\psi_0(\eta)$, $\nu_0(\eta)$, and $\phi_0(\eta)$ each form two families of "universal functions" depending only on the power law of the body.

The order-ϵ system of equations is given as follows:

Continuity:

$$\psi_0\phi_1' + \left(\psi_0' + \frac{\sigma}{\eta}\psi_0\right)\phi_1 - (\eta - \phi_0)\psi_1' + \left[\phi_0' + \frac{\sigma}{\eta}\phi_0 + 2\left(\frac{1 - m}{m}\right)\right]\psi_1 = 0 \tag{11a}$$

Longitudinal momentum:

$$(\eta - \phi_0)\nu_1' + \eta\frac{F_1'}{\psi_0} - \frac{1}{\psi_0^2}\left[\eta F_0' + 2\left(\frac{1 - m}{m}\right)F_0\right]\psi_1 - \nu_0'\phi_1 = 0 \tag{11b}$$

Lateral momentum:

$$(\eta - \phi_0)\phi_1' - \frac{F_1'}{\psi_0} + \frac{F_0'}{\psi_0^2}\psi_1 - \left[\phi_0' + \left(\frac{1 - m}{m}\right)\right]\phi_1 = 0 \tag{11c}$$

Energy:

$$(\eta - \phi_0)\left[\left(\gamma\frac{\psi_1'}{\psi_0} - \frac{F_1'}{F_0}\right) - \left(\gamma\frac{\psi_0'}{\psi_0^2}\psi_1 - \frac{F_0'}{F_0^2}F_1\right)\right]$$

$$- 2\left(\frac{1 - m}{m}\right)\left(\gamma\frac{\psi_1}{\psi_0} - \frac{F_1}{F_0}\right) - \left(\gamma\frac{\psi_0'}{\psi_0} - \frac{F_0'}{F_0}\right)\phi_1 = 0 \tag{11d}$$

These equations are the same as Kubota's (ref. 3) first-order perturbation for shock-wave strength, except that (again) he omitted the longitudinal-momentum equation since it is uncoupled from the rest. They can be solved numerically by using the results of the zero-order solutions. The resulting similarity functions $F_1(\eta)$, $\psi_1(\eta)$, $\nu_1(\eta)$, and $\phi_1(\eta)$ are also universal, like the zero-order functions, in that they depend only on m as a parameter. References 3, 4, and 13 contain the results of numerical solutions of the zero-order and the order-ϵ equations.

The remaining four equations form the order-δ^2 system, which has not been determined previously, and are given as follows:

Continuity:

$$\psi_0\phi_2' + \left(\psi_0' + \frac{\sigma}{\eta}\psi_0\right)\phi_2 - (\eta - \phi_0)\psi_2' + \left[\phi_0' + \frac{\sigma}{\eta}\phi_0 - 2\left(\frac{1-m}{m}\right)\right]\psi_2$$

$$- \eta\nu_0\psi_0' - \left[\eta\nu_0' + 2\left(\frac{1-m}{m}\right)\nu_0\right]\psi_0 = 0 \qquad (12a)$$

Longitudinal momentum:

$$(\eta - \phi_0)\nu_2' + \eta\frac{F_2'}{\psi_0} + 4\left(\frac{1-m}{m}\right)\left(\nu_2 + \frac{F_2}{\psi_0}\right) - \frac{1}{\psi_0^2}\left[\eta F_0' + 2\left(\frac{1-m}{m}\right)F_0\right]\psi_2$$

$$- \nu_0'\phi_2 + \nu_0\left[\eta\nu_0' + 2\left(\frac{1-m}{m}\right)\nu_0\right] = 0 \qquad (12b)$$

Lateral momentum:

$$(\eta - \phi_0)\phi_2' - \frac{F_2'}{\psi_0} + \frac{F_0'}{\psi_0^2}\psi_2 - \left[\phi_0' - 3\left(\frac{1-m}{m}\right)\right]\phi_2 + \left[\eta\phi_0' + \left(\frac{1-m}{m}\right)\phi_0\right]\nu_0 = 0 \qquad (12c)$$

Energy:

$$(\eta - \phi_0)\left[\left(\gamma\frac{\psi_2'}{\psi_0} - \frac{F_2'}{F_0}\right) - \left(\gamma\frac{\psi_0'\psi_2}{\psi_0^2} - \frac{F_0'F_2}{F_0^2}\right)\right] + 2\left(\frac{1-m}{m}\right)\left(\gamma\frac{\psi_2}{\psi_0} - \frac{F_2}{F_0}\right)$$

$$- \left(\gamma\frac{\psi_0'}{\psi_0} - \frac{F_0'}{F_0}\right)\phi_2 - \left[2\left(\frac{1-m}{m}\right) - \eta\left(\gamma\frac{\psi_0'}{\psi_0} - \frac{F_0'}{F_0}\right)\right]\nu_0 = 0 \qquad (12d)$$

Except for additional terms corresponding to the order-δ^2 terms retained in the normalized flow equations (2), these equations are very similar to the order-ϵ equations; many of the coefficients are the same, and the only body shape parameter that appears is m. The similarity functions $F_2(\eta)$, $\psi_2(\eta)$, $\nu_2(\eta)$, and $\phi_2(\eta)$, which form the solutions to these equations, will, therefore, be families of universal functions in the same sense as

the other solutions are. Furthermore, just as the order-ϵ equations are independent of the body slenderness perturbation (in δ^2), these equations are independent of the shock-wave strength perturbation (in ϵ). Thus, application of these equations to determine the body slenderness perturbation of the zero-order small-disturbance similar solutions neither requires nor excludes application of the equations for the shock-strength perturbation at the same time.

Since the order-ϵ solutions have been found previously and are not needed to get the order-δ^2 solutions, they will not be considered further. (Ref. 14 shows that the order-δ^2 and order-ϵ boundary conditions are also mutually independent.) All subsequent development will assume $\epsilon << \delta^2$ so that $\epsilon = O(\delta^4) << 1$; all terms of order-$\delta^4$ or smaller will be neglected.

Boundary Conditions

Shock wave.- The boundary conditions at the shock wave are determined by the oblique-shock relations (eqs. (3)). By using the expression for $R(\xi)$ (eq. (6)), these equations in their expanded form (eqs. (4)) become (omitting the order-ϵ terms):

$$\left.\begin{aligned} p_s &= \frac{2}{\gamma+1} m^2 \xi^{-2(1-m)} + \delta^2 \frac{2}{\gamma+1}\left[2\left(\frac{3m-2}{m}\right)a_2 - 1\right] m^4 \xi^{-4(1-m)} + O(\delta^4) \\ \rho_s &= \frac{\gamma+1}{\gamma-1} + O(\delta^4) \\ u_s &= -\frac{2}{\gamma+1} m^2 \xi^{-2(1-m)} - \delta^2 \frac{2}{\gamma+1}\left[2\left(\frac{3m-2}{m}\right)a_2 - 1\right] m^4 \xi^{-4(1-m)} + O(\delta^4) \\ v_s &= \frac{2}{\gamma+1} m \xi^{-(1-m)} + \delta^2 \frac{2}{\gamma+1}\left[\left(\frac{3m-2}{m}\right)a_2 - 1\right] m^3 \xi^{-3(1-m)} + O(\delta^4) \end{aligned}\right\} \tag{13}$$

Comparing these equations term-by-term with equations (7) determines the boundary conditions for the similarity functions at the shock wave ($\eta = \eta_s$):

$$\left.\begin{aligned} F_0(\eta_s) &= \frac{2}{\gamma+1} & \nu_0(\eta_s) &= -\frac{2}{\gamma+1} \\ \psi_0(\eta_s) &= \frac{\gamma+1}{\gamma-1} & \phi_0(\eta_s) &= \frac{2}{\gamma+1} \end{aligned}\right\} \tag{14a}$$

$$
\left.
\begin{aligned}
F_2(\eta_s) &= \frac{2}{\gamma+1}\left[2\left(\frac{3m-2}{m}\right)a_2 - 1\right] \\
\psi_2(\eta_s) &= 0 \\
\nu_2(\eta_s) &= -\frac{2}{\gamma+1}\left[2\left(\frac{3m-2}{m}\right)a_2 - 1\right] \\
\phi_2(\eta_s) &= \frac{2}{\gamma+1}\left[\left(\frac{3m-2}{m}\right)a_2 - 1\right]
\end{aligned}
\right\} \tag{14b}
$$

Note that the shock-wave displacement constant a_2 initially is unknown. It depends on the parameter m and is to be found in satisfying the boundary condition at the body surface as part of the solution of the flow equations.

Body surface.- The boundary conditions at the body surface are determined by requiring zero mass flow through the surface. Thus, the mass flow normal to the surface (fig. 2) is given by

$$\bar{\rho}_b \bar{v}_b \cos \theta_b - \bar{\rho}_b \bar{u}_b \sin \theta_b = 0 \tag{15}$$

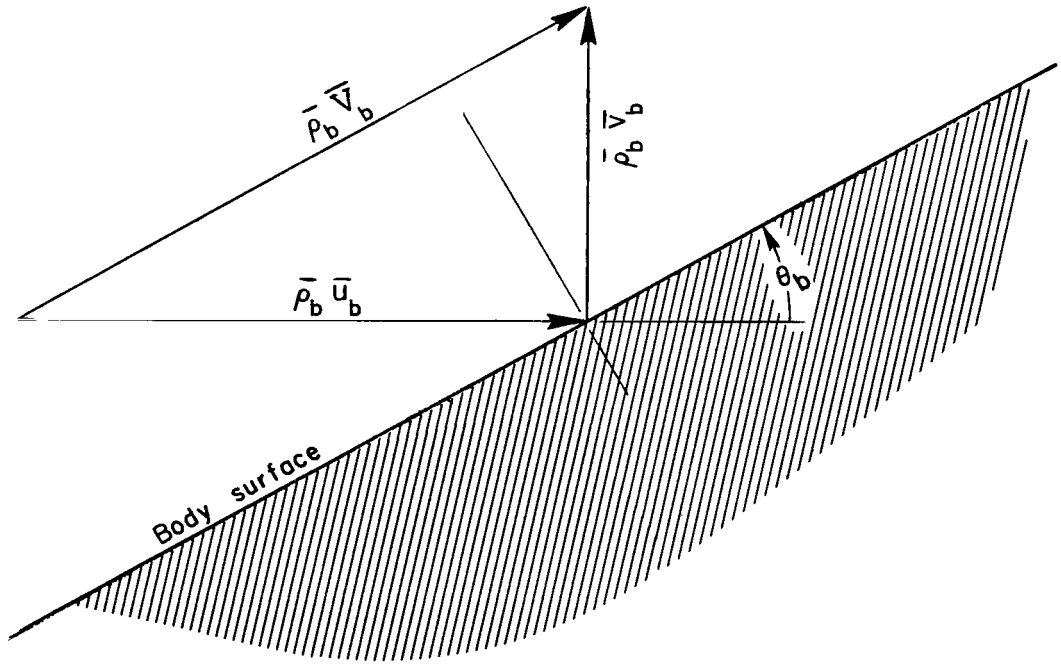

Figure 2.- Vector diagram of flow at the body surface.

Or, in the normalized variables,

$$v_b = \frac{1}{\delta}\left(1 + \delta^2 u_b\right) \tan \theta_b \tag{16}$$

Now,

$$\tan \theta_b = \frac{d\bar{r}_b}{d\bar{x}} = \delta \eta_b m \xi^{-(1-m)}$$

Putting this into equation (16) along with the expressions for u and v in terms of the similarity functions from equations (7) gives the relation

$$\left[\phi_0(\eta_b) - \eta_b\right] m \xi^{-(1-m)} + \delta^2 \left[\phi_2(\eta_b) - \eta_b \nu_0(\eta_b)\right] m^3 \xi^{-3(1-m)} + O(\delta^4) = 0$$

The resulting boundary conditions at the body surface are

$$\left.\begin{aligned} \phi_0(\eta_b) - \eta_b &= 0 \\ \phi_2(\eta_b) - \eta_b \nu_0(\eta_b) &= 0 \end{aligned}\right\} \tag{17}$$

SOLUTION OF EQUATIONS

The similarity forms of the flow equations (10) and (12) with the boundary conditions at the shock wave (eqs. (14)) and at the body surface (eqs. (17)) are sufficient to determine completely an order-δ^2 solution for the flow field. Although there is no general analytic form, solutions can be found by integrating numerically for each value of the power-law exponent m (with σ set equal to either 0 or 1). This section first puts the equations into the form required for the numerical integration; then, it develops methods for overcoming certain difficulties in applying the boundary conditions; and, finally, it describes the numerical-integration method.

General Scheme of Solution

The general scheme for obtaining the solution is to begin at the shock $\eta = \eta_s$, where the boundary conditions are known, and to integrate the similarity functions numerically toward the body, which is known to be reached when the zero-order boundary condition is satisfied; that is, $\eta = \eta_b$ when $\phi_0(\eta) = \eta$. The derivatives of the similarity functions, used for the integration, are found by solving the flow equations for them algebraically.

Thus, from the zero-order equations (10), the derivatives are

$$\left.\begin{aligned}
F_0'(\eta) &= \frac{\psi_0}{\gamma - (\eta - \phi_0)^2 \frac{\psi_0}{F_0}} \left\{ \gamma \left(\frac{1 - m}{m} \right) \phi_0 - (\eta - \phi_0) \left[\gamma \frac{\sigma}{\eta} \phi_0 - 2 \left(\frac{1 - m}{m} \right) \right] \right\} \\
\psi_0'(\eta) &= \frac{\psi_0}{\gamma} \left\{ \frac{F_0'}{F_0} + 2 \left(\frac{1 - m}{m} \right) \Big/ (\eta - \phi_0) \right\} \\
\nu_0'(\eta) &= \frac{-1}{\eta - \phi_0} \left\{ \eta \frac{F_0'}{\psi_0} + 2 \left(\frac{1 - m}{m} \right) \left(\nu_0 + \frac{F_0}{\psi_0} \right) \right\} \\
\phi_0'(\eta) &= \frac{1}{\eta - \phi_0} \left\{ \frac{F_0'}{\psi_0} - \left(\frac{1 - m}{m} \right) \phi_0 \right\}
\end{aligned}\right\} \qquad (18)$$

The derivatives of the order-δ^2 functions, from equations (12), are

$$\begin{aligned}
\phi_2'(\eta) = \Bigg\{ & \left[(\eta - \phi_0) \frac{\psi_0}{F_0} \left(3 \frac{1 - m}{m} - \phi_0' \right) - \gamma \frac{\sigma}{\eta} - \frac{F_0'}{F_0} \right] \\
& + (\eta - \phi_0) \left(\frac{\psi_2}{\psi_0} - \frac{F_2}{F_0} \right) \frac{F_0'}{F_0} + 2 \left(\frac{1 - m}{m} \right) \frac{F_2}{F_0} + \gamma \eta \nu_0' \\
& + \left[(\eta - \phi_0) \frac{\psi_0}{F_0} \left(\eta \phi_0' + \frac{1 - m}{m} \phi_0 \right) + \eta \frac{F_0'}{F_0} + 2(\gamma + 1) \left(\frac{1 - m}{m} \right) \right] \Bigg\} \\
& \div \left[\gamma - (\eta - \phi_0)^2 \frac{\psi_0}{F_0} \right]
\end{aligned} \qquad (19a)$$

$$F_2' = \psi_0\left\{(\eta - \phi_0)\phi_2' + \left[3\left(\frac{1-m}{m}\right) - \phi_0'\right]\phi_2 + \left[\eta\phi_0' + \left(\frac{1-m}{m}\right)\phi_0\right]\nu_0\right\} + \frac{F_0'}{\psi_0}\psi_2 \tag{19b}$$

$$\psi_2' = \frac{1}{\eta - \phi_0}\left\{\left[\phi_0' + \frac{\sigma}{\eta}\phi_0 - 2\left(\frac{1-m}{m}\right)\right]\psi_2 + \psi_0\phi_2'\right.$$

$$\left. + \left(\psi_0' + \frac{\sigma}{\eta}\psi_0\right)\phi_2 - 2\left(\frac{1-m}{m}\right)\nu_0\psi_0 - \eta\left(\nu_0\psi_0' + \psi_0\nu_0'\right)\right\} \tag{19c}$$

$$\nu_2' = \frac{1}{\eta - \phi_0}\left\{\nu_0'\phi_2 - \frac{\eta}{\psi_0}F_2' - 4\left(\frac{1-m}{m}\right)\nu_2\right.$$

$$\left. + \frac{F_0}{\psi_0}\left[\left(2\,\frac{1-m}{m} + \eta\,\frac{F_0'}{F_0}\right)\frac{\psi_2}{\psi_0} - 4\left(\frac{1-m}{m}\right)\frac{F_2}{F_0}\right]\right\} \tag{19d}$$

Two major difficulties must be overcome in order to apply the scheme of integrating these equations from the shock to the body. One difficulty is the singularity at the body surface apparent from the fact that the denominators of some of the terms of these equations approach zero as the independent variable η approaches the surface value η_b. (From eqs. (17), $\phi_0 - \eta \to 0$ as $\eta \to \eta_b$.) It is overcome for the zero-order functions by using an approximate analytic solution developed by Mirels (ref. 4). Mirels' results at the body surface can be expressed as

$$\left.\begin{aligned}
&\left(\frac{\eta_b}{\eta}\right)^{1+\sigma} \approx 1 - \frac{\gamma}{\gamma - \beta}\left(\frac{\eta - \phi_0}{\eta}\right)\left[1 + \frac{\beta(\eta - \phi_0)}{2(2\gamma - \beta)}\,\frac{\psi_0}{F_0}\left(\frac{\eta_b}{\eta}\right)^{1-\sigma}\right] \\
&F_0(\eta_b) \approx F_0(\eta) - \frac{\beta}{2}\eta_b(\eta - \phi_0)\psi_0\left(\frac{\eta}{\eta_b}\right)^{\sigma} \\
&\psi_0(\eta_b) = 0
\end{aligned}\right\} \tag{20}$$

These relations are correct to the order of θ_0^2, where $\theta_0 = \eta^\sigma\psi_0(\eta - \phi_0)$ is a stream-function similarity variable. Since $\theta_0 \to 0$ as $\eta \to \eta_b$, they apply near the body

surface. The order-δ^2 similarity functions F_2, ψ_2, ϕ_2, and ν_2 are calculated at the body by extrapolation. The extrapolation curve (chosen for convenience) is the cubic in η passing through three of the computed points of the function and having its second derivative equal to zero at the body surface. The points used to define the cubic were the computed point nearest the body surface and two previous points chosen so as to make the distance between points larger than the distance between the last point and the body.

The second of the two major difficulties is associated with the fact that the problem is a two-point boundary-value problem. This difficulty is manifest in the need to choose the correct value of the shock-wave displacement parameter a_2 (eq. (6)) at the beginning of the integration in order to satisfy the order-δ^2 boundary condition at the body surface at the end of the integration. The measures taken to deal with this difficulty are described in the following section.

Methods for Determining the Constant a_2

Since the constant a_2 is initially undetermined, the value of the order-δ^2 shock-wave similarity ordinate $\eta_s = 1 + \delta^2 a_2 m^2 \xi^{-2(1-m)}$ is unknown and cannot be used to begin the integration toward the body surface. Also, using the shock ordinate would reintroduce the longitudinal distance ξ, which is undesirable. The use of the zero-order shock ordinate $\eta = 1$ as the starting point for the integration avoids these two problems but requires that the boundary conditions be transferred from $\eta = \eta_s$, where they are known, to $\eta = 1$. This transfer is made by using the Taylor series expansions of the similarity flow variables about the point $\eta = \eta_s$. Applying the Taylor series expansion to equations (7) (with terms of order ϵ neglected) and evaluating at $\eta = 1$ gives to order δ^2:

$$p(\xi,1) = F_0(\eta_s) m^2 \xi^{-2(1-m)} + \delta^2 \left[F_2(\eta_s) - a_2 F_0'(\eta_s) \right] m^4 \xi^{-4(1-m)}$$

$$\rho(\xi,1) = \psi_0(\eta_s) + \delta^2 \left[\psi_2(\eta_s) - a_2 \psi_0'(\eta_s) \right] m^2 \xi^{-2(1-m)}$$

$$u(\xi,1) = \nu_0(\eta_s) m^2 \xi^{-2(1-m)} + \delta^2 \left[\nu_2(\eta_s) - a_2 \nu_0'(\eta_s) \right] m^4 \xi^{-4(1-m)}$$

$$v(\xi,1) = \phi_0(\eta_s) m \xi^{-(1-m)} + \delta^2 \left[\phi_2(\eta_s) - a_2 \phi_0'(\eta_s) \right] m^3 \xi^{-3(1-m)}$$

Comparing the results of evaluating these equations (by using eqs. (18) for the derivatives and eqs. (14) for the boundary conditions at η_s) with the results of evaluating equations (7) at $\eta = 1$ directly gives the transferred boundary conditions at $\eta = 1$:

$$
\left.
\begin{aligned}
&F_0(1) = \phi_0(1) = \frac{2}{\gamma + 1} \qquad \psi_0(1) = \frac{\gamma + 1}{\gamma - 1} \qquad \nu_0(1) = \frac{-2}{\gamma + 1} \\
&F_2(1) = \frac{2}{\gamma + 1}\left\{2\left[\left(\frac{3m - 2}{m}\right) - \left(\frac{1 - m}{m}\right)\left(\frac{2\gamma - 1}{\gamma - 1}\right) + \frac{\sigma\gamma}{\gamma + 1}\right]a_2 - 1\right\} \\
&\psi_2(1) = -\frac{2}{\gamma - 1}\left[3\left(\frac{1 - m}{m}\right)\left(\frac{\gamma + 1}{\gamma - 1}\right) - \sigma\right]a_2 \\
&\nu_2(1) = -\frac{2}{\gamma + 1}\left\{2\left[\left(\frac{3m - 2}{m}\right) - \left(\frac{1 - m}{m}\right)\frac{1}{\gamma - 1} + \frac{\sigma\gamma}{\gamma + 1}\right]a_2 - 1\right\} \\
&\phi_2(1) = \frac{2}{\gamma + 1}\left\{\left[\left(\frac{3m - 2}{m}\right) - 3\left(\frac{1 - m}{m}\right) + 2\,\frac{\sigma\gamma}{\gamma + 1}\right]a_2 - 1\right\}
\end{aligned}
\right\} \qquad (21)
$$

Iteration method.- These transferred boundary conditions provide a definite starting position for the integration toward the body, but the constant a_2 must still be determined by one of two methods. The more obvious one is to guess the value of a_2, integrate toward the body (using the method given in the previous section to reach the surface), test the order-δ^2 boundary condition at the surface, and repeat using improved guesses until the surface boundary condition is satisfied closely enough. Improved guesses for this iteration method were made by using the method of chords, a finite difference approximation to the well-known Newton-Raphson method.

Decomposition method.- The other method for determining a_2 takes advantage of the linearity of the equations in the order-δ^2 functions, which allows superposition of solutions. It was used by Kubota (ref. 3) and Mirels (ref. 4) in obtaining their results and is applied in a similar manner here. Each of the order-δ^2 similarity functions is decomposed into a linear combination in the parameter a_2; for example,

$$\left.\begin{aligned} F_2(\eta) &= F_{2,a}(\eta)a_2 + F_{2,c}(\eta) \\ \psi_2(\eta) &= \psi_{2,a}(\eta)a_2 + \psi_{2,c}(\eta) \end{aligned}\right\} \tag{22}$$

These decomposed variables are then substituted into the order-δ^2 flow equations so that the continuity equation (12a), for example, becomes

$$\left\{\psi_0\phi_{2,a}' + \left(\psi_0' + \frac{\sigma}{\eta}\psi_0\right)\phi_{2,a} - (\eta - \phi_0)\psi_{2,a}' + \left[\phi_0' + \frac{\sigma}{\eta}\phi_0 + 2\left(\frac{1-m}{m}\right)\right]\psi_{2,a}\right\} a_2$$

$$+ \left\{\psi_0\phi_{2,c}' + \left(\psi_0' + \frac{\sigma}{\eta}\psi_0\right)\phi_{2,c} - (\eta - \phi_0)\psi_{2,c}' + \left[\phi_0' + \frac{\sigma}{\eta}\phi_0 + 2\left(\frac{1-m}{m}\right)\right]\psi_{2,c}\right.$$

$$\left. - \eta\nu_0\psi_0' - \left[\eta\nu_0' + 2\left(\frac{1-m}{m}\right)\nu_0\right]\psi_0\right\} = 0$$

Splitting each of the equations obtained in this way into two separate equations (by setting the term containing a_2 and the other term each equal to zero) produces a system of equations in the subscript-c functions and a system in the subscript-a functions. The system in the subscript-c functions is identical to the original system of equations (12). The system in the subscript-a functions is the same except that the inhomogeneous terms (i.e., the terms that do not contain an order-δ^2 function or its derivative) do not appear. These two systems of equations have different sets of boundary conditions. In order to obtain them, the boundary conditions at $\eta = 1$ (eqs. (21)) are decomposed by comparisons with equations (22), thus giving

$$F_{2,a}(1) = \frac{4}{\gamma+1}\left[\left(\frac{3m-2}{m}\right) - \left(\frac{1-m}{m}\right)\left(\frac{2\gamma-1}{\gamma-1}\right) + \frac{\sigma\gamma}{\gamma+1}\right] \qquad F_{2,c}(1) = -\frac{2}{\gamma+1}$$

$$\psi_{2,a}(1) = -\frac{2}{\gamma-1}\left[3\left(\frac{1-m}{m}\right)\left(\frac{\gamma+1}{\gamma-1}\right) - \sigma\right] \qquad \psi_{2,c}(1) = 0$$

$$\nu_{2,a}(1) = -\frac{4}{\gamma+1}\left[\left(\frac{3m-2}{m}\right) - \left(\frac{1-m}{m}\right)\left(\frac{1}{\gamma-1}\right) + \frac{\sigma\gamma}{\gamma+1}\right] \qquad \nu_{2,c}(1) = \frac{2}{\gamma+1}$$

$$\phi_{2,a}(1) = \frac{2}{\gamma + 1}\left[\left(\frac{3m - 2}{m}\right) - 3\left(\frac{1 - m}{m}\right) + 2\frac{\sigma\gamma}{\gamma + 1}\right] \qquad \phi_{2,c}(1) = -\frac{2}{\gamma + 1}$$

Beginning at $\eta = 1$ with these boundary conditions, the decomposed system of equations (which is now 12 linear differential equations in 12 unknowns) is integrated toward the body. The boundary condition at the surface, expressed in terms of the surface values of the decomposed functions, is (from eqs. (17))

$$\phi_{2,a}(\eta_b)a_2 + \phi_{2,c}(\eta_b) - \eta_b\nu_0(\eta_b) = 0$$

Solving for a_2 gives

$$a_2 = \frac{\eta_b\nu_0(\eta_b) - \phi_{2,c}(\eta_b)}{\phi_{2,a}(\eta_b)} \tag{23}$$

This value of a_2 is now used to recombine the decomposed similarity functions by using relations such as equations (22).

Once these functions have been computed for any value of the body power-law exponent m (with $\sigma = 0$ or 1), they can be used to calculate the complete flow field about any such body as long as it is slender enough that $\delta^4 << 1$ and the Mach number is large enough that $\epsilon \equiv \frac{1}{M_\infty{}^2\delta^2} << 1$. The appendix shows how to apply the solutions to a given power-law body.

Description of the Numerical Method

Two separate computer programs were written to integrate equations (18) and (19); one uses the iterative method and the other uses the decomposition method for obtaining the value of a_2. These computer programs use a standard integration subroutine employing the fourth-order Runge-Kutta formula supplemented by a Richardson's extrapolation. This subroutine halves or doubles the integration step size automatically in order to meet specified local truncation-error criteria.

For the present computations the initial step size (in η), which was also the chosen maximum step size, was 2^{-7} (0.0078125). Generally, the step size decreased to less than 2^{-15} near the body. At each step, estimates of η_b and $F_0(\eta_b)$ were computed by use of equations (20). When both estimates agreed to within 1.0×10^{-9} on successive steps, the estimates were accepted as the actual values of η_b and $F_0(\eta_b)$ and the values of the other functions at the body were computed by the cubic extrapolation. The

maximum extrapolation distance for $m \neq 1$ was 0.000174 in η. The iteration for a_2 was considered to have converged when the order-δ^2 boundary condition at the surface (eqs. (17)) was satisfied to within 0.5×10^{-10}.

DISCUSSION OF RESULTS

Zero-Order Functions

The methods given in the previous section have been used to compute the zero-order and order-δ^2 similarity functions for a number of cases. (All are for $\gamma = 1.4$, representing an ideal diatomic gas.) The figures presenting the functions were generated by plotting machines directly from the computed results. The slight waviness which may be noticeable in some of the figures is a result of this computer-aided plotting process; however, the curves at all points on the plots are accurate to within ±0.1 percent of the full-scale values.

The zero-order similarity functions F_0, ψ_0, ϕ_0, and ν_0 are shown for several values of the power-law exponent m in figure 3 for two-dimensional flow ($\sigma = 0$) and in figure 4 for axially symmetric flow ($\sigma = 1$). Numerical values of the functions are given in tables I and II. These functions agree with the same functions calculated by Kubota (ref. 3), Mirels (refs. 4 and 6), and Townsend (ref. 13).

The pressure function F_0 and the lateral-velocity function ϕ_0 are seen to be smooth and well behaved from the zero-order shock location ($\eta = 1$) to the body surface. Note that the body-surface values of ϕ_0 lie on the line $\phi_0 = \eta$ in accordance with the zero-order boundary condition (eqs. (17)). However, the density function ψ_0 and the longitudinal-velocity function ν_0 exhibit different types of singular behavior at the body surface for $m \neq 1$: ψ_0 goes to zero, and ν_0 goes toward minus infinity. This singularity at the body surface is an entropy-layer effect caused by the blunt nose of the body for $m < 1$. Van Dyke (ref. 16, page 186) notes the same singular behavior at the surface in a small-disturbance solution for hypersonic flow over a blunted wedge and observes that it occurs because the zero-order solution "is not a valid first approximation in the entropy layer." For the power-law body the effect is confined to a narrow region since the very high curvature in the nose area (infinite at $x = 0$) reduces the body slope rapidly. For example, when $m = 0.80$ and $\delta = 0.5$, the slope decreases from infinite to less than 1.0 before $\bar{x}/\bar{l} = 0.006$.

Van Dyke (ref. 16) uses the method of matched asymptotic expansions to obtain a uniformly valid analytic solution for the blunted wedge. Adaptation of that method to the similarity-solution problem for power-law bodies probably would extend the solutions to the body surface; but, the application is complicated by the similar solutions being in

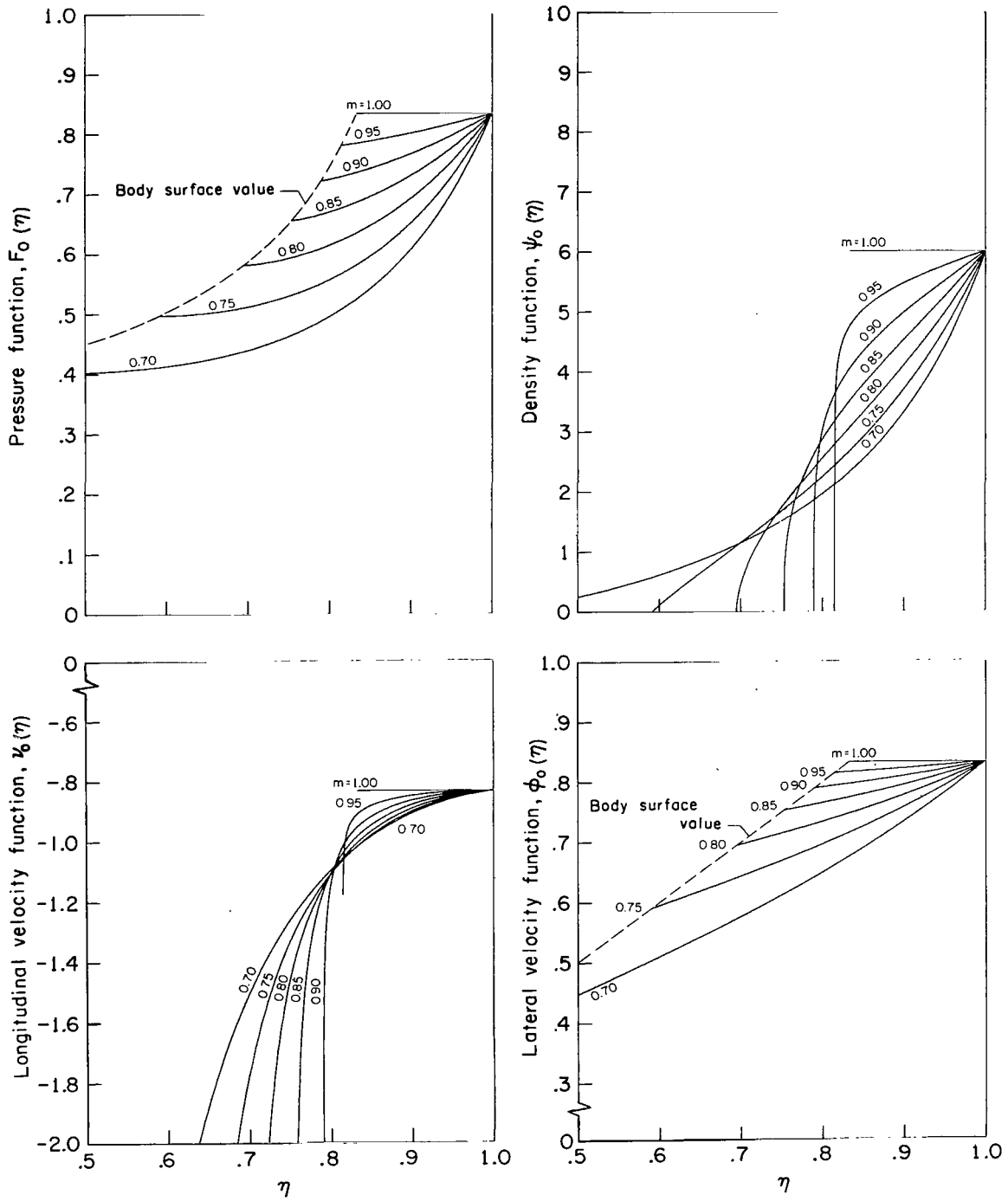

Figure 3.- Zero-order similarity functions for two-dimensional flow ($\sigma = 0$).

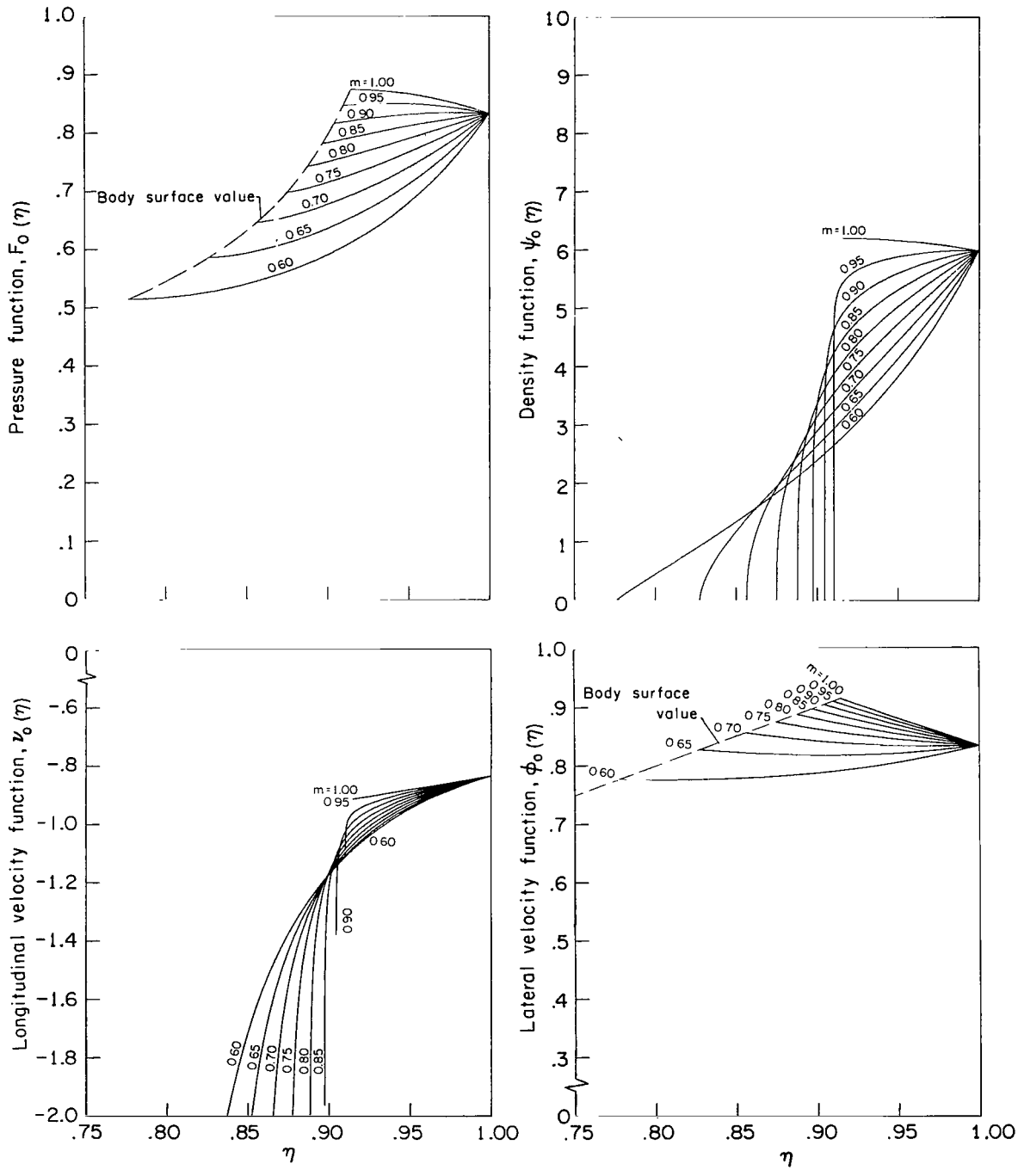

Figure 4.- Zero-order similarity functions for axisymmetric flow ($\sigma = 1$).

numerical form. Mirels (ref. 4) recognized the singularity at the body surface even though he did not calculate the longitudinal velocity function, which exhibits the singular behavior. He avoided the singularity by developing an approximate analytic solution and using it to obtain surface values of the zero-order functions (eqs. (20)).

Shock-Displacement Constant

The variation of the calculated order-δ^2 shock-wave displacement constant a_2 with the power-law exponent m is shown in figure 5 for both two-dimensional and axisymmetric bodies. The calculations made by using the iterative method for obtaining a_2 gave essentially the same values as were obtained by the decomposition method (eq. (23)). However, the results from both methods are characterized by a singular discontinuity in a_2 which has no physical counterpart in the actual flow about power-law bodies. This singularity, which occurs near $m = 0.817$ for $\sigma = 0$ and near $m = 0.653$ for $\sigma = 1$ (two-dimensional and axially symmetric flow, respectively), represents a sudden decrease in the distance from the shock to the body as the power-law decreases, followed by a jump to a large distance across the discontinuity. Since this behavior is physically unrealistic, it must be produced by the mathematical processes (analytical and numerical) used to obtain the solutions.

The upper part of figure 5 shows that the singularity is associated with a zero in the denominator of equation (23). Since there is a nearby zero in the numerator of this equation, it appears possible that the singularity in the quotient a_2 occurs because the zeros in the numerator and denominator are displaced relative to one another by accumulated errors in the numerical solution. (Coincidence of the zeros would make a_2 mathematically indeterminate at that point but could allow a continuous variation of a_2 with m, from which the value at the indeterminate point could be inferred.) To test this possibility, additional calculations were made by reducing the step size, reducing the range of the extrapolation, and, finally, extrapolating the whole of equation (23) rather than just the separate parts. The results of these calculations indicated that the position of the singularity and the values of a_2 for m greater than that at the singularity were virtually unaffected by the numerical procedure. The singularity was even unaffected by a complete reformulation of the problem in terms of momentum components instead of velocity components and by a change in extrapolation mode (ref. 14), although these changes did produce large changes in the computed value of a_2 for m less than that at the singularity (dashed line in fig. 5). Thus, removing the singularity would require a radical change in the mathematical process rather than simply changing parameters in the numerical integration and extrapolation schemes. For example, logarithmic terms might be required in the shock-wave and flow-variable expansions (eqs. (6) and (7)).

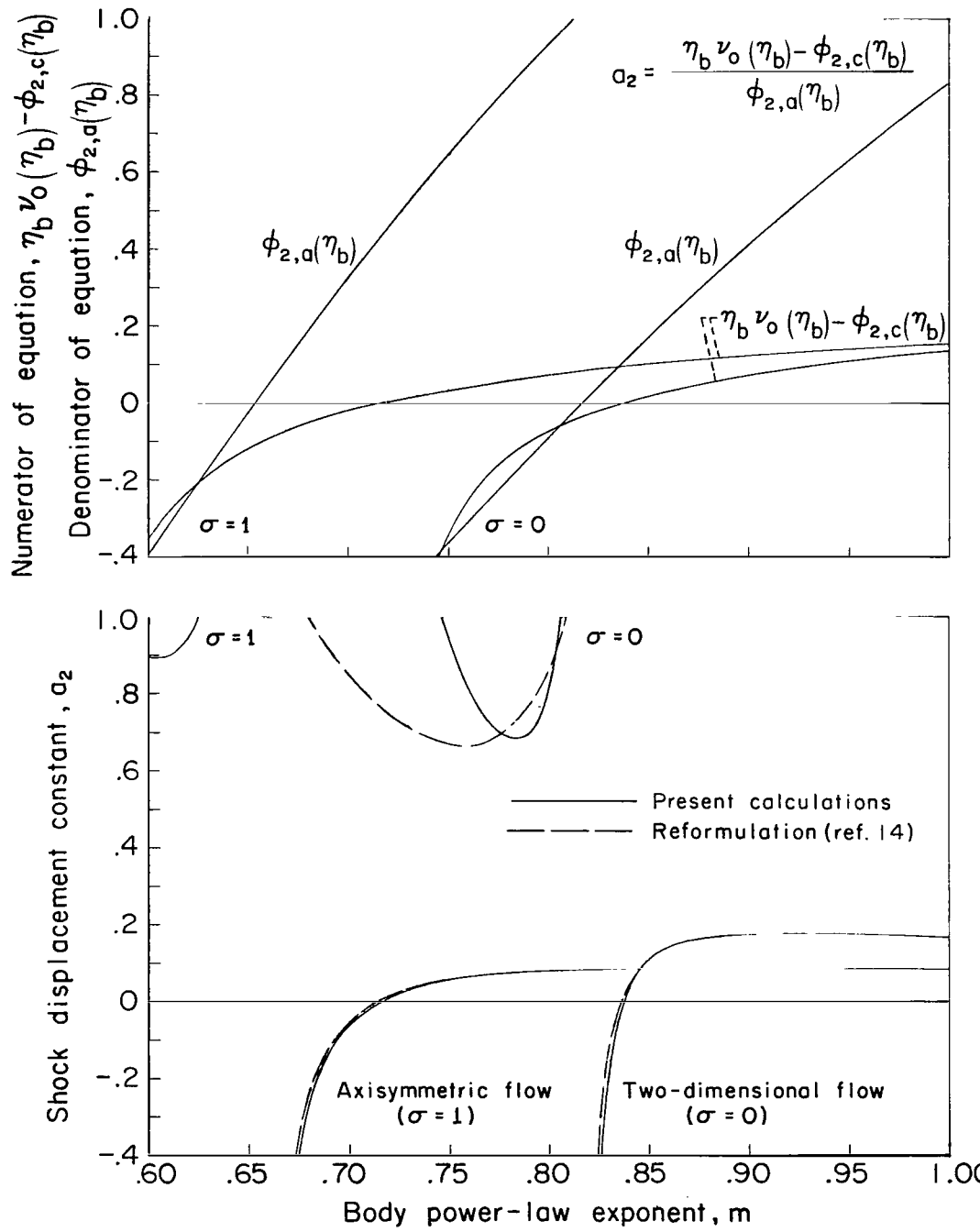

Figure 5.- Variation of shock displacement constant a_2 with body power-law exponent m.

The results of the present calculations should be reasonably good for body power-law exponents outside the range of significant influence from the singularity. Based on figure 5, the range for good results is about $0.85 \leqq m \leqq 1.0$ for the two-dimensional flow ($\sigma = 0$) and $0.75 \leqq m \leqq 1.0$ for the axisymmetric flow ($\sigma = 1$). Note that this is a more restricted range than that for which similarity solutions exist $\left(\frac{2}{3 + \sigma} < m \leqq 1\right.$ (ref. 2)$\Big)$ or for which entropy-layer effects are less than first order $\left(\frac{2(\gamma + 1)}{(3 + \sigma)\gamma + 2} < m \leqq 1\right.$ (ref. 17)$\Big)$.

Order-δ^2 Functions

The order-δ^2 similarity functions F_2, ψ_2, ν_2, and ϕ_2 are shown in figure 6 for two-dimensional flow ($\sigma = 0$) and in figure 7 for axisymmetric flow ($\sigma = 1$). The results shown were obtained by using the decomposition technique for calculating the shock-displacement constant a_2 (eq. (23)), but essentially identical results were also obtained by using iteration. Numerical values of the functions are given in tables I and II. These order-δ^2 functions are seen to have some differences in behavior from the zero-order functions described previously. One obvious difference is that the curves describing these functions do not all emanate from a single point at $\eta = 1$. The variation at $\eta = 1$ is due to the variation of the order-δ^2 boundary conditions at the shock with the body power law m and to the transfer of the boundary conditions from $\eta = \eta_s$ to $\eta = 1$.

All of the order-δ^2 functions except the pressure function F_2 show singular behavior at the body surface for $m < 1$. These singularities in the order-δ^2 functions are a result of the entropy layer, just as in the case of the zero-order function ν_0. In effect, the order-δ^2 functions try to compensate for the large deviation of the zero-order longitudinal-velocity function at the surface, and so they become singular there also. The effect of the singularity is to make the order-δ^2 solution inapplicable at the body surface (except for the particular case of $m = 1$, for which the body does not have a blunt nose). However, the singularity should not affect the solution away from the surface, where the similarity functions are of order unity, so long as the constant a_2 is correctly determined. Furthermore, the behavior of the order-δ^2 similarity function for the pressure F_2 is quite regular all the way to the surface. Thus, the body surface pressure can be calculated to order-δ^2 by using this function; however, the results must be suspect until checked against experiment or more exact results.

It is because of the singular behavior of the similarity functions that the numerical integration cannot proceed all the way to the body surface. Neither do the extrapolations follow the singular functions in giving values at the surface; so, the calculated surface values of these functions do not represent the actual values of the singular functions,

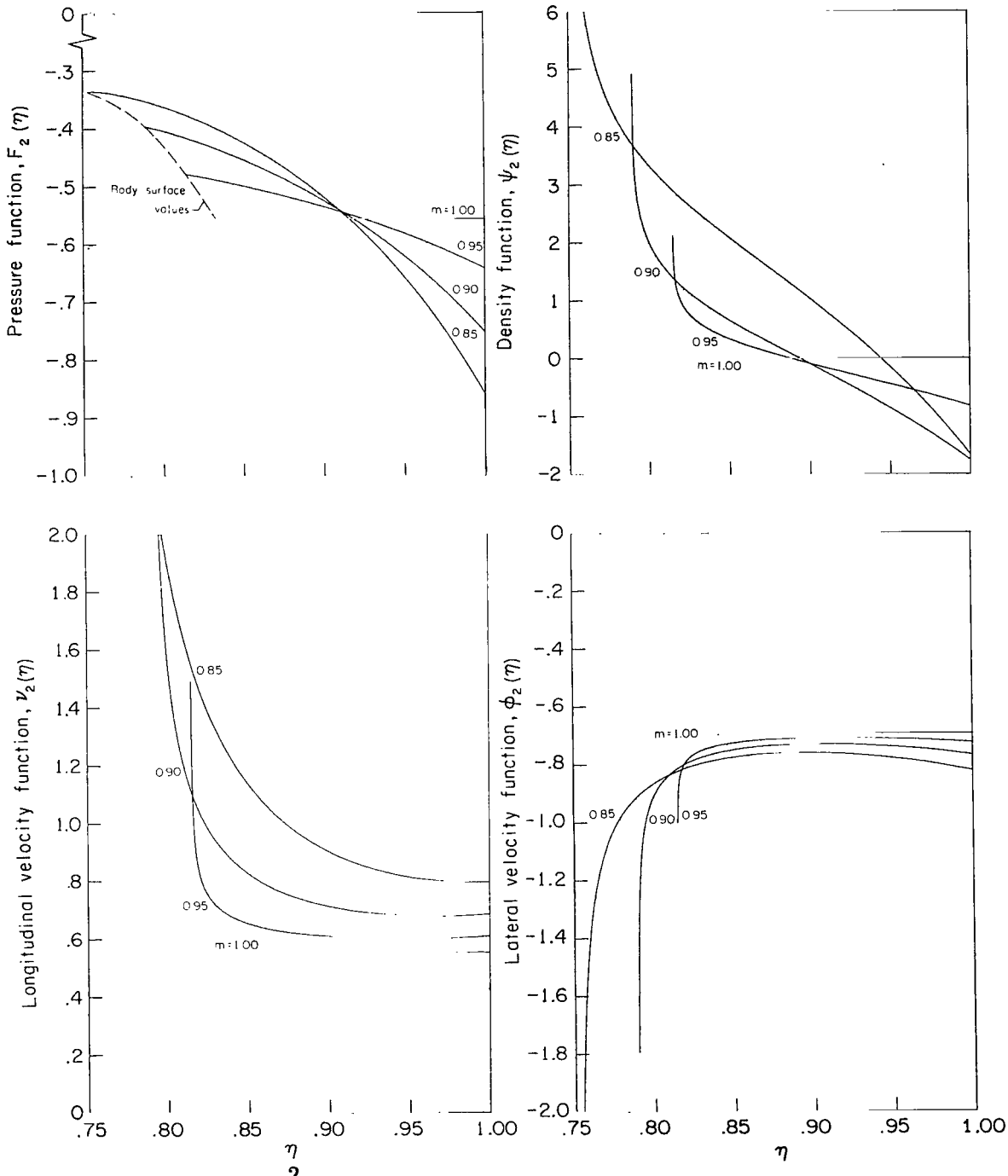

Figure 6.- Order-δ^2 similarity functions for two-dimensional flow ($\sigma = 0$).

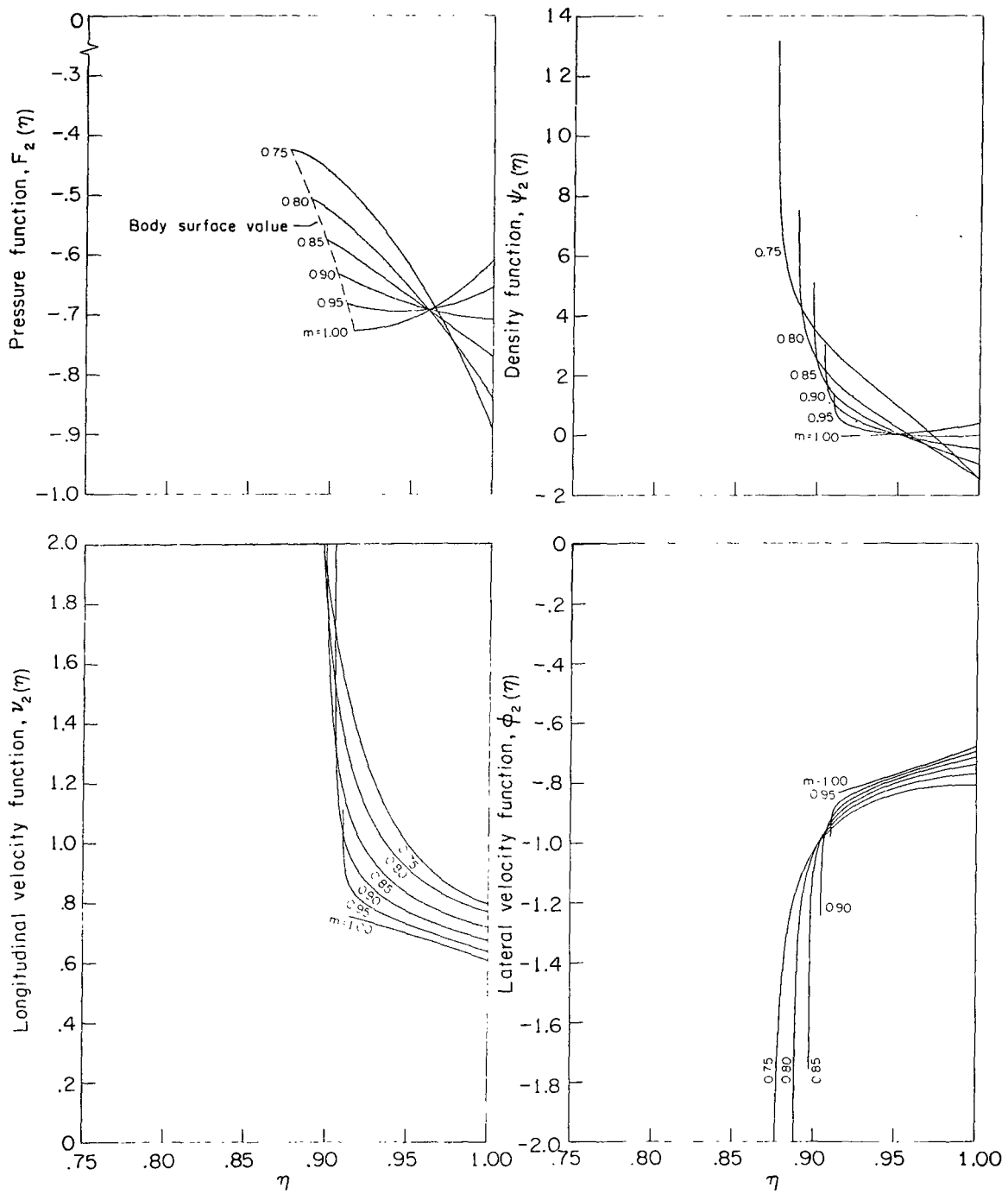

Figure 7.- Order-δ^2 similarity functions for axisymmetric flow ($\sigma = 1$).

which go to either plus or minus infinity at the surface. To the extent that they are useful for determining the value of a_2, the extrapolations can be considered as providing a limiting process for this constant.

Region of Validity of the Solutions

Three basic assumptions were required in order to obtain the hypersonic similarity solutions for power-law bodies: (1) The body is slender enough that terms of order-δ^4 are negligible compared to unity; (2) the shock wave about the body is strong enough that terms of order $\epsilon \equiv 1/\delta^2 M_\infty^2$ are negligible compared to unity; and (3) the Mach number is large compared to unity. (The second of these can be relaxed to $\epsilon^2 \ll 1$ if the first-order solution in ϵ is applied.) However, even when these three assumptions are met overall for a particular power-law body, they generally are not all met in particular local regions.

The first assumption, $\delta^4 \ll 1$, is obviously violated in the nose region of all blunt bodies, such as the power-law bodies for $m < 1$. Thus, the similarity solutions cannot be expected to apply at the nose of these bodies. But, the order-δ^2 solutions should be particularly useful in providing an improved solution a moderate distance behind the nose. As mentioned in the previous section, the violation of the slender-body assumption by the blunt nose is also the cause of the singularities in the order-δ^2 functions at the body surface. Therefore, because the first assumption is violated at the nose, the order-δ^2 solution does not apply at the body surface.

The strong shock assumption, $\epsilon \ll 1$, is violated wherever the shock-wave angle approaches the Mach angle, $\sin^{-1}(1/M_\infty)$. Unless the Mach number is extremely large, the shock wave will become weak far downstream from the nose of the body, and the similarity solutions will not apply in that region.

The similarity solutions apply, then, in an intermediate region from behind the nose to somewhere in the vicinity of the base of the body, and, in the case of the order-δ^2 solution, only outside of the singularity at the body surface. The boundaries of this region depend on the Mach number and on the power-law exponent and slenderness of the body. Decreasing the Mach number or increasing the slenderness of the body tends to weaken the shock; decreasing the power-law exponent increases the nose bluntness but weakens the shock at the rear of the body. In any case, the boundaries of the region in which the solutions apply are not sharply defined but depend on the accuracy required in the results.

Comparison With Other Solutions

The only exact solutions available for comparison with the similarity solutions are those for flow over cones and wedges, corresponding to a power-law exponent of $m = 1$.

(A finite-difference calculation for $m = 0.75$ will be discussed in the next section.) Since the zero-order and order-δ^2 similarity solutions do not contain any Mach number dependence, the most appropriate comparison is at the hypersonic limit, $M_\infty \to \infty$. Results from the similarity solutions, in terms of the physical flow variables, are compared in figure 8 with the exact solutions for flow over a range of wedge angles at infinite Mach number. This flow, of course, is uniform behind the straight oblique shock wave, as indicated by the solutions for $m = 1$ in figures 3 and 6. In figure 9, results from the similarity solutions are compared with the exact solutions for flow over circular cones. Figures 8(a) and 9(a) show the variation of shock-wave angle with the body surface angle and include exact results from several Mach numbers in addition to $M_\infty = \infty$. The other parts of figures 8 and 9 show the variations with the body surface angle of the pressure coefficient $\bar{p}/\bar{q}_\infty$, the velocity $\bar{V}/\bar{u}_\infty = \sqrt{\bar{u}^2 + \bar{v}^2}\Big/\bar{u}_\infty$, and the velocity components $\bar{u}/\bar{u}_\infty$ and $\bar{v}/\bar{u}_\infty$ in the uniform flow behind the shock wave (fig. 8) and at the body surface (fig. 9). The similarity results are found from equations (6) and (7) with $m = 1$ as described in the appendix. The exact results are found from the oblique-shock relations in the two-dimensional case and from the charts of reference 15 and tables of reference 18 in the axisymmetric case.

Figures 8 and 9 show that for $m = 1$ the zero-order similarity solution agrees well with the exact solution for body surface angles up to about $\theta_b \approx 12^\circ$, whereas the order-$\delta^2$ solution agrees well up to body angles of about $\theta_b = 20^\circ$. As can be seen at the bottom of the figures, these cone or wedge angles correspond to slenderness-parameter values of about $\delta \approx 0.2$ and $\delta \approx 0.4$. The shock-wave angles calculated by similarity theory agree especially well with the exact solutions for infinite Mach number. In fact, over a substantial range of body angles the agreement is very good with the exact results for Mach numbers down to twelve. The similarity results for the magnitude of the velocity also show good agreement for relatively large body angles (figs. 8(c) and 9(c)). Since the error is larger for the velocity components (figs. 8(d) and 9(d)), it must come mainly from error in predicting the direction of the velocity vector. This error in direction is shown in the upper part of figures 8(c) and 9(c), where it is compared to the curves $\delta^2\theta_b$ and $-\delta^4\theta_b$. These curves represent the order of error expected from neglecting terms of order-δ^2 and of order-δ^4, respectively. The error actually occurring is seen to be very close to that which was expected. It should be noted that this error in the direction of the velocity vector corresponds to an error in satisfying the boundary condition that there is no flow through the body surface. That is, the velocity component normal to the surface $\bar{V} \sin\left[\tan^{-1}\left(\frac{v_b}{u_b}\right) - \theta_b\right]$ should be zero. Figures 8(c) and 9(c) show that this boundary condition is satisfied to order-δ^2 by the order-δ^2 similarity solution for $m = 1$.

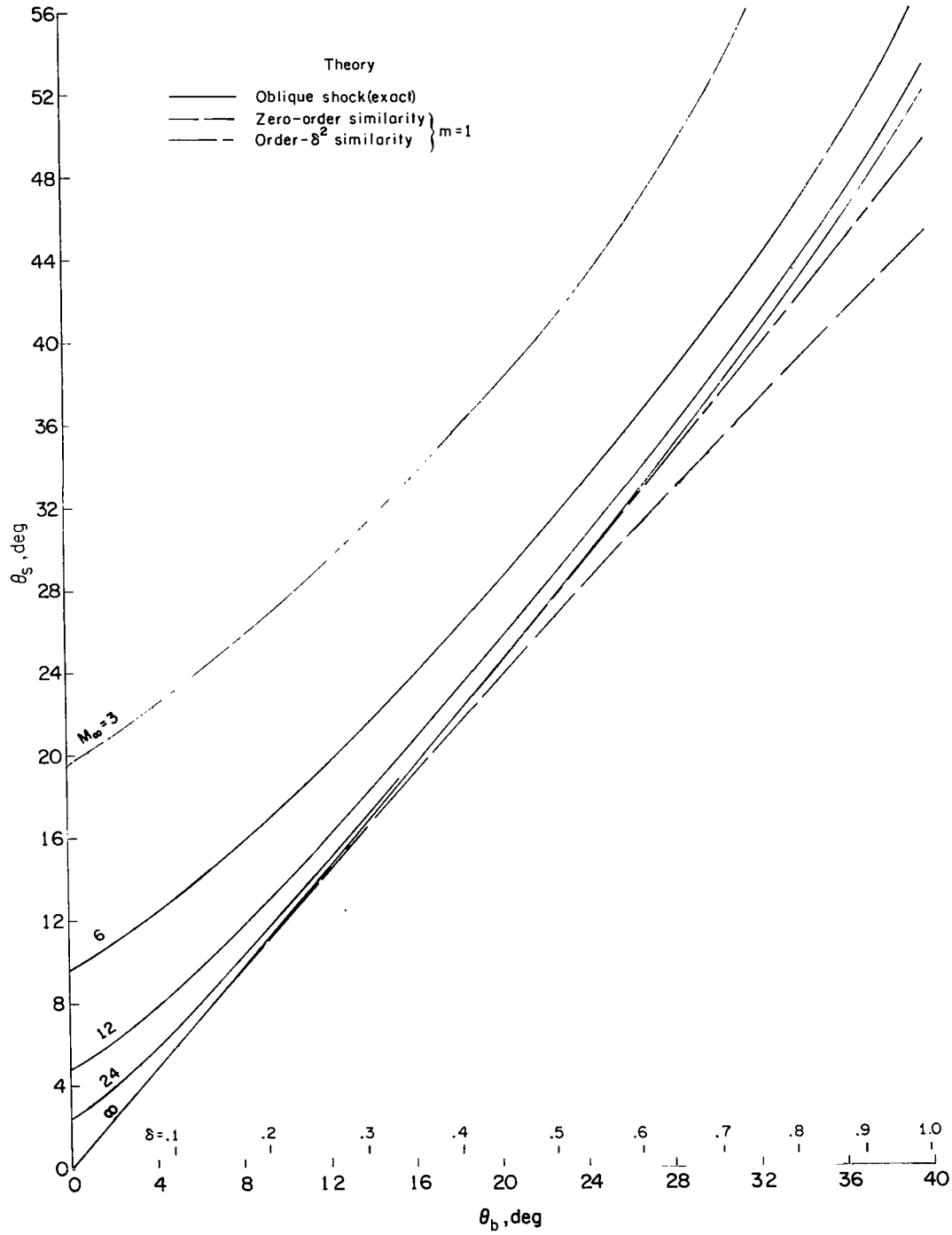

(a) Shock-wave angle θ_s.

Figure 8.- Comparison of similarity solution for $m = 1$ with exact solution for flow over a wedge at $M_\infty = \infty$.

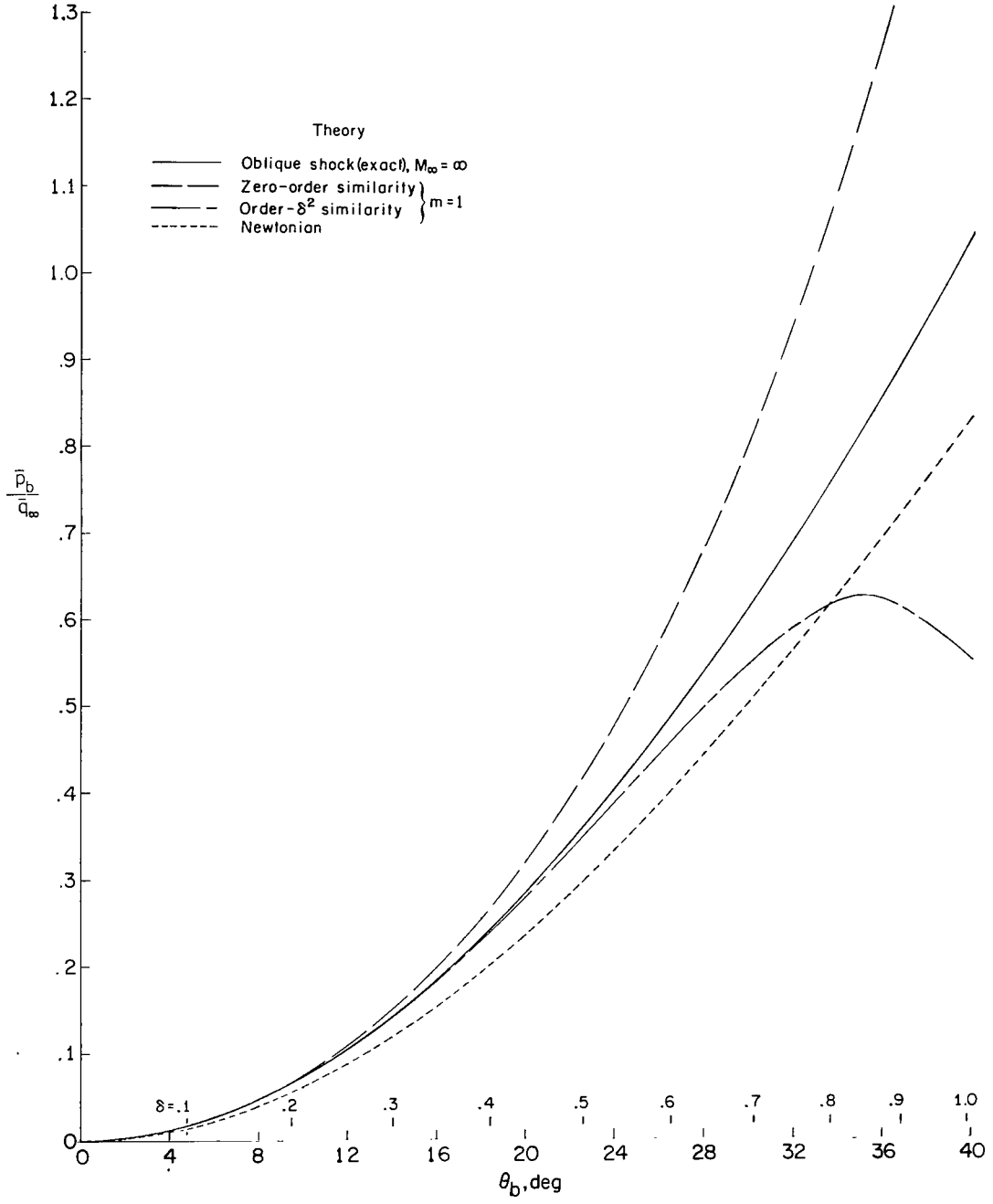

(b) Pressure $\bar{p}/\bar{q}_\infty$.

Figure 8.- Continued.

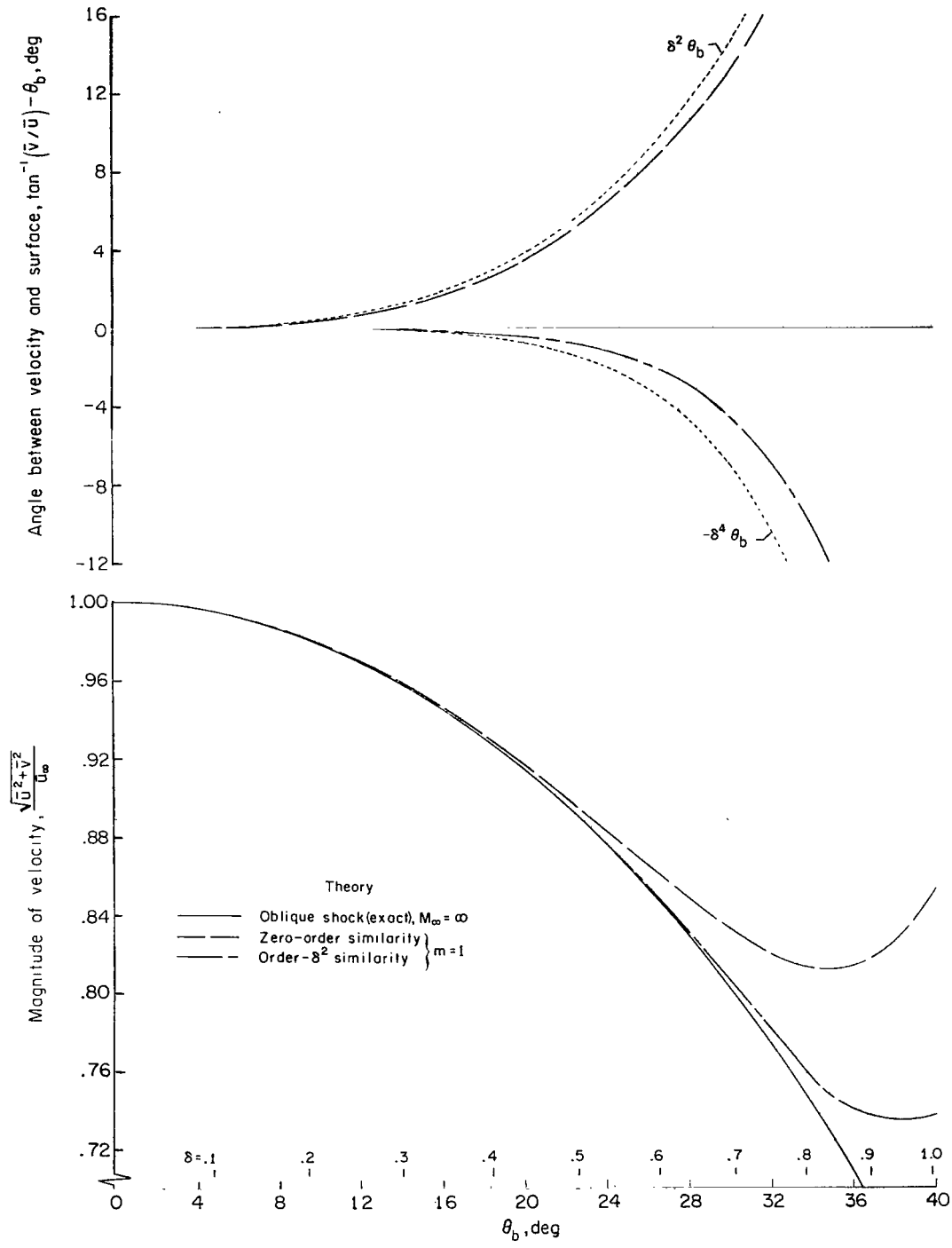

(c) Magnitude and direction of the velocity vector.

Figure 8.- Continued.

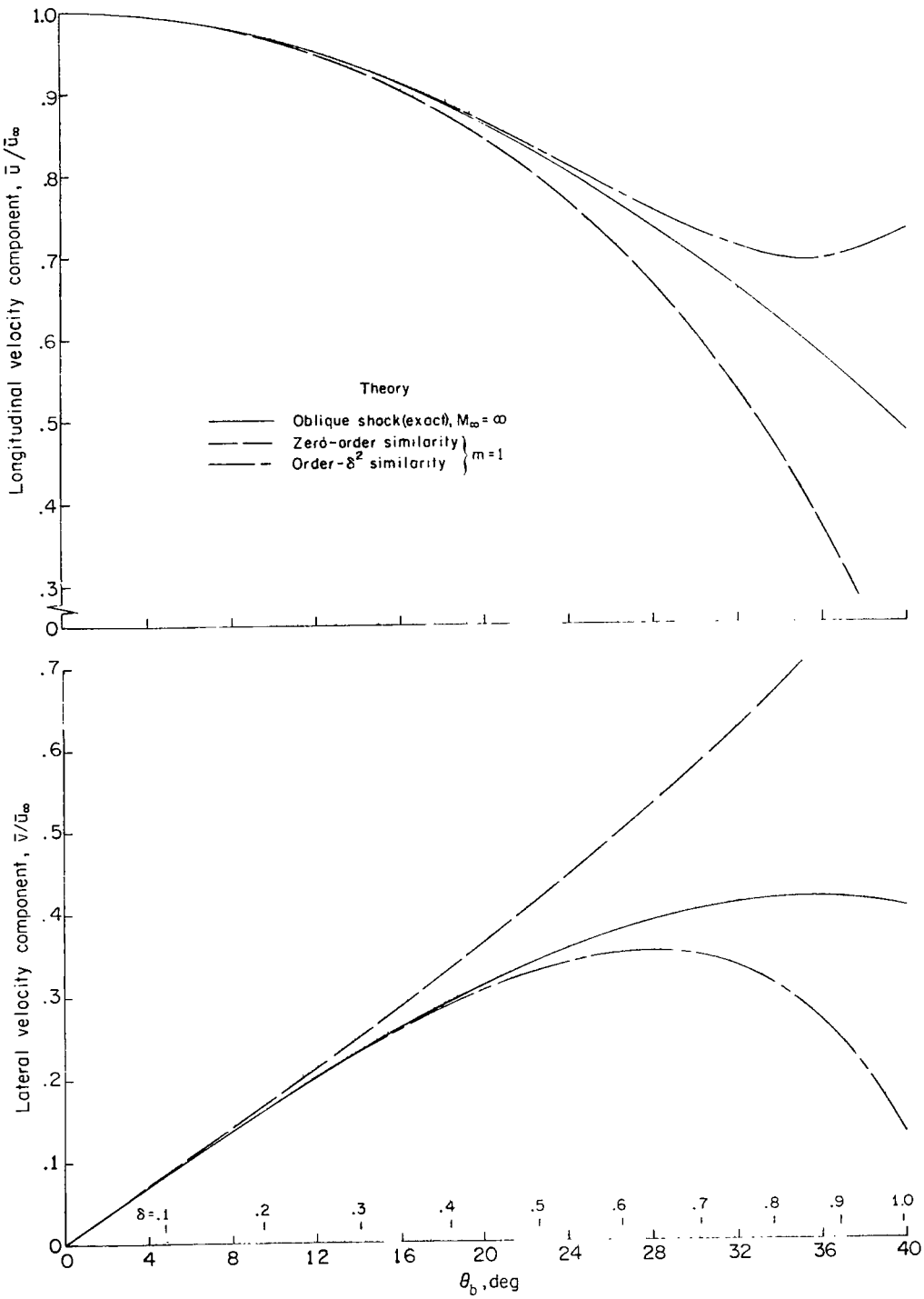

(d) Velocity components.

Figure 8.- Concluded.

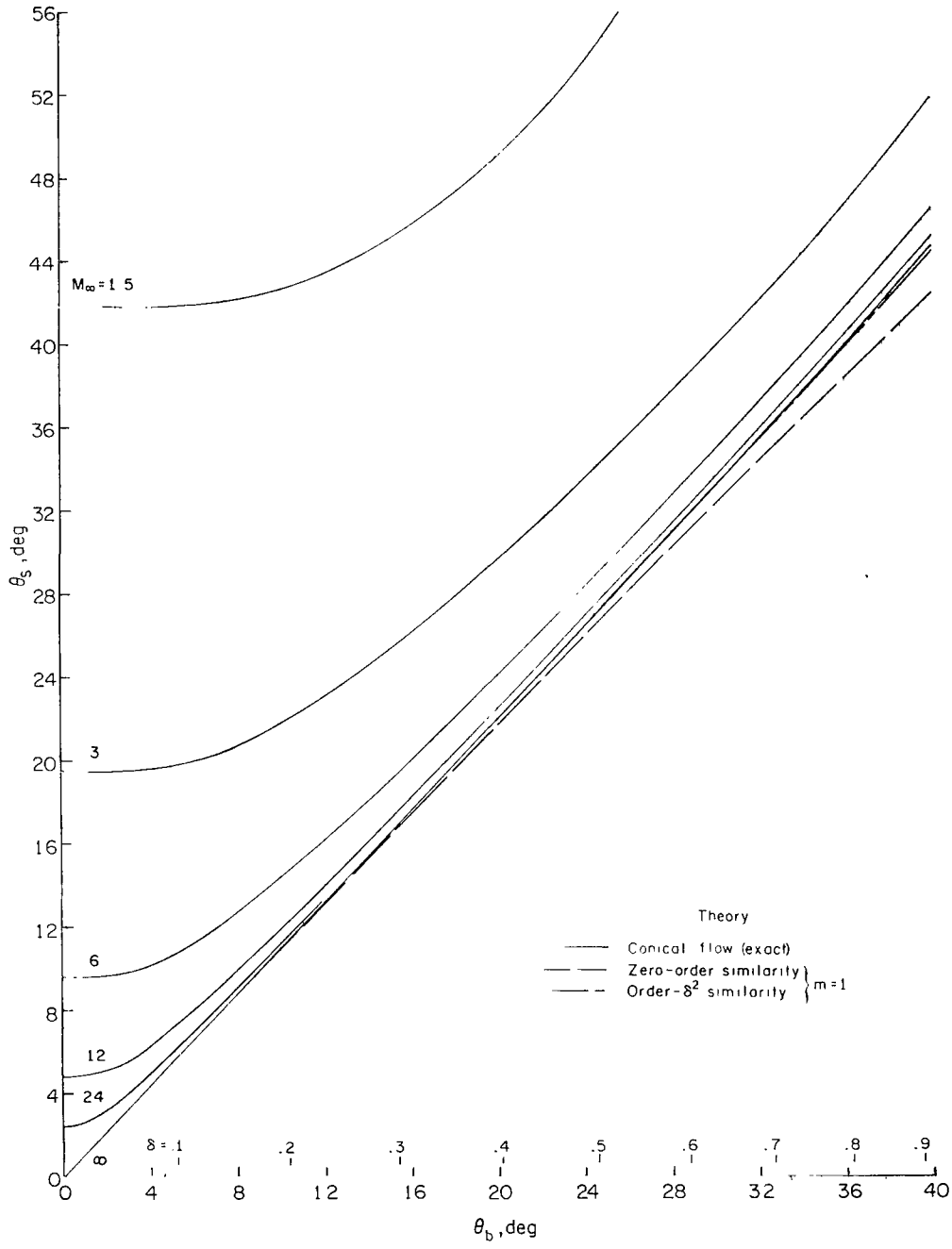

(a) Shock-wave angle θ_s.

Figure 9.- Comparison of similarity solution for $m = 1$ with exact solution for flow over a circular cone at $M_\infty = \infty$.

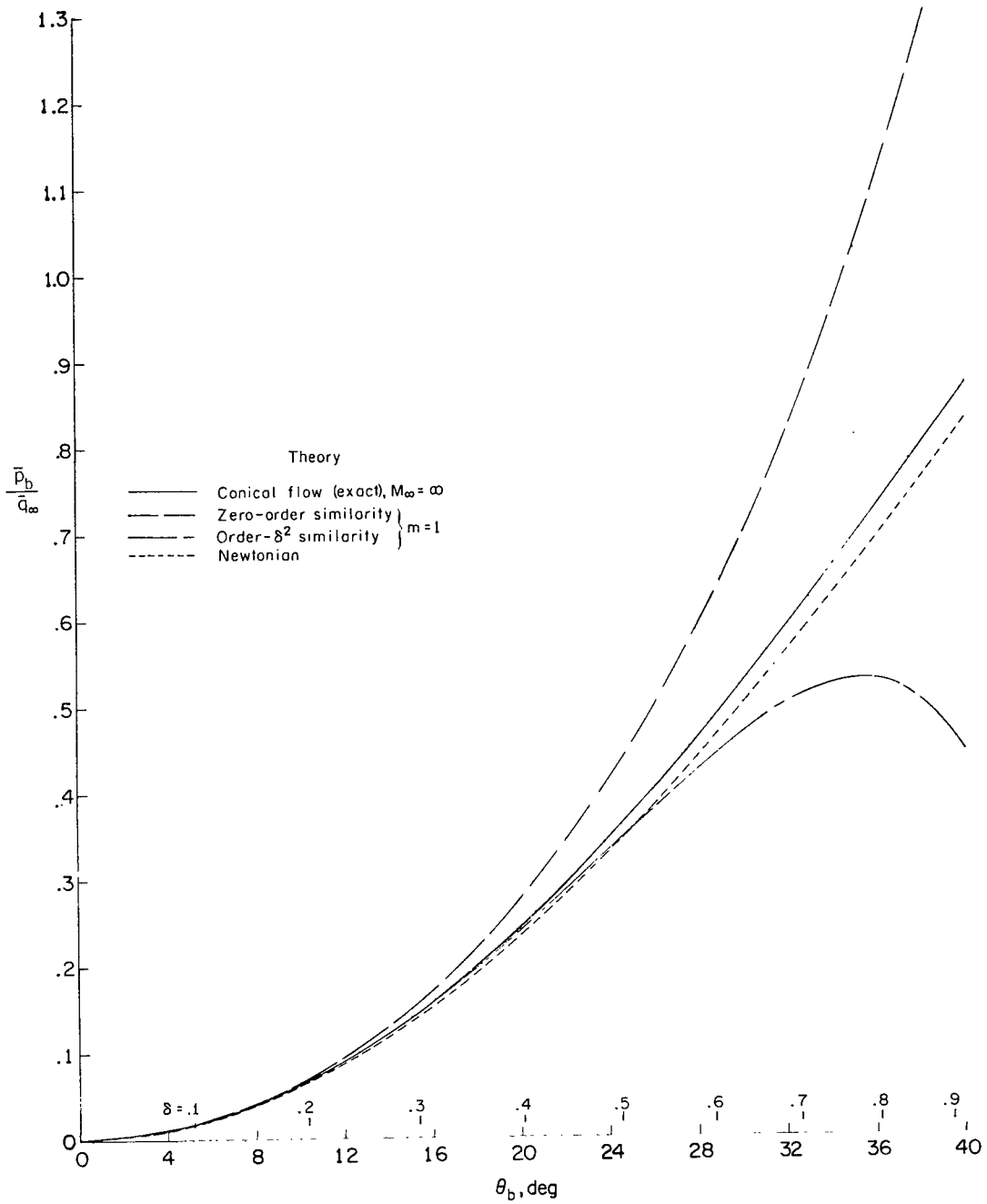

(b) Surface pressure $\bar{p}_b/\bar{q}_\infty$.

Figure 9.- Continued.

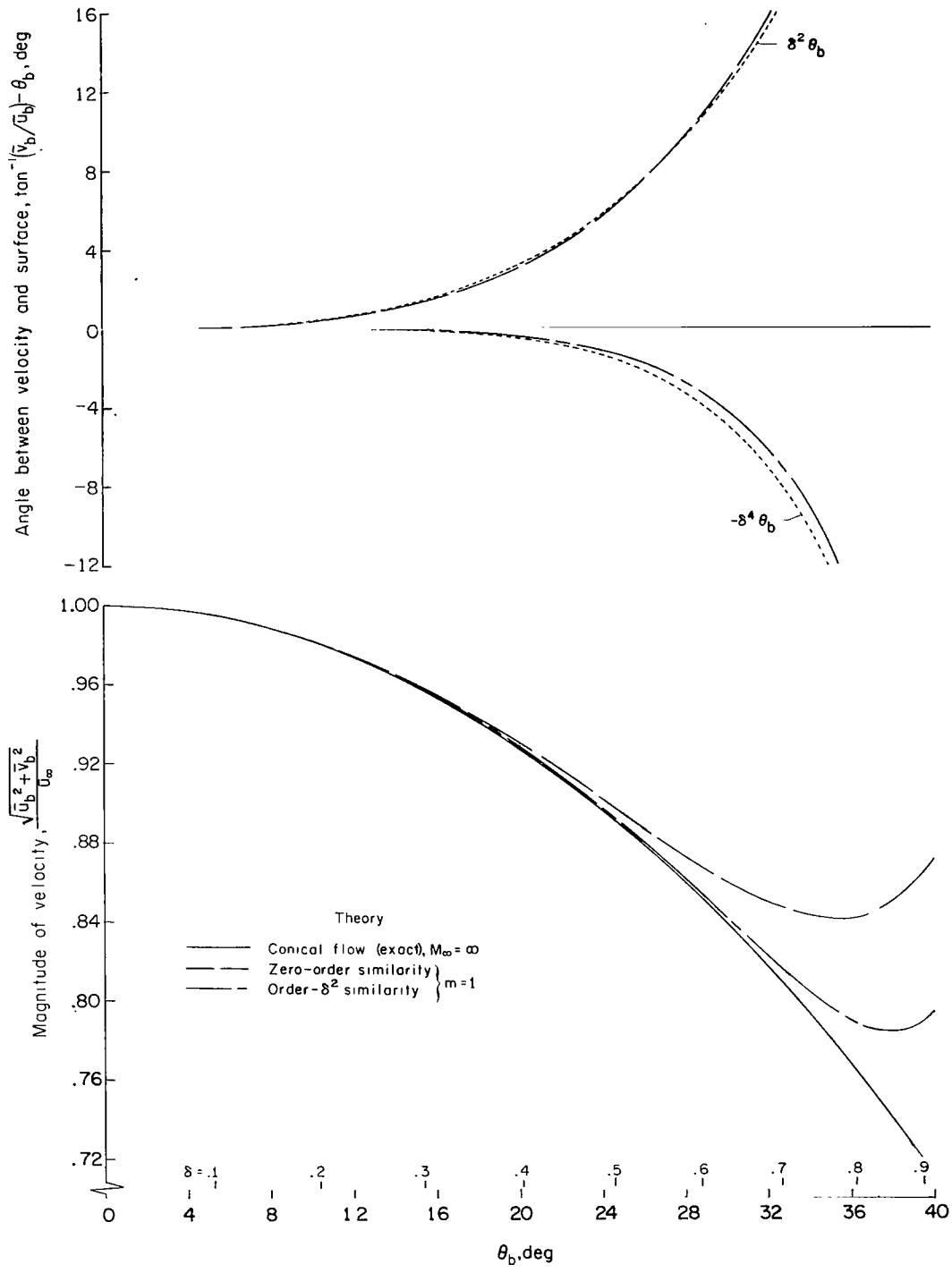

(c) Magnitude and direction of the velocity vector at the body surface.

Figure 9.- Continued.

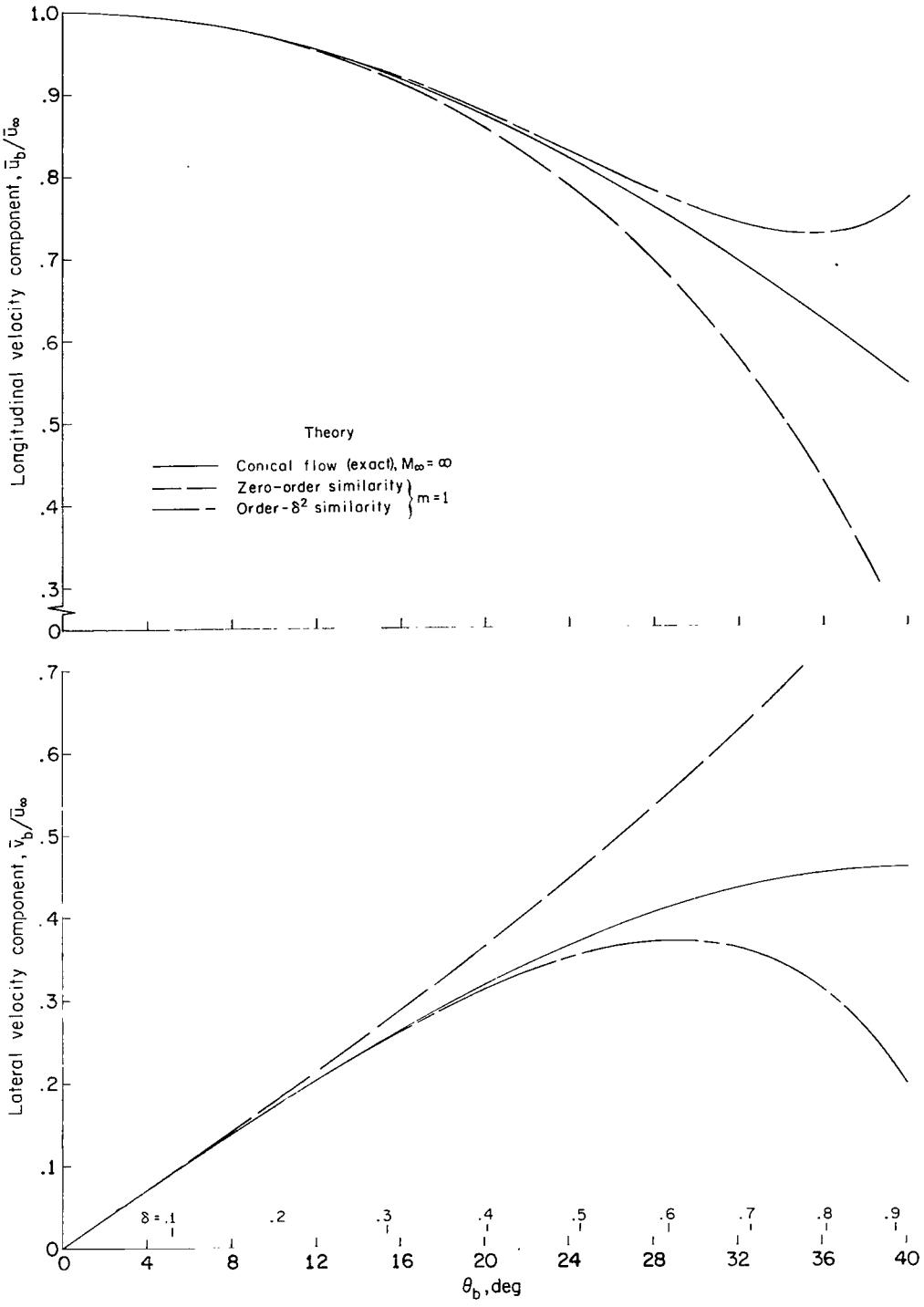

(d) Surface velocity components.

Figure 9.- Concluded.

In figures 8(b) and 9(b), the pressure coefficients are compared also with the Newtonian prediction: $\bar{p}/\bar{q}_\infty = 2 \sin^2\theta_b$. The Newtonian prediction is much more accurate for the conical flows (fig. 9(b)) than for the wedge flows (fig. 8(b)); however, even in the conical case the order-δ^2 similarity solution is closer to the exact solution for values of the similarity parameter $\delta \leqq 0.5$.

In figure 10, the variation of the flow variables from the shock to the body is shown for three values of the power-law exponent, $m = 1.0$, 0.85, and 0.75. The pressure, density, and velocity components, calculated from the axisymmetric zero-order and order-δ^2 similarity solutions, are shown at $\bar{x}/\bar{l} = 0.5$ for a similarity parameter value of $\delta = 0.4$. Note that the zero-order results begin at $\eta = 1$, which is the zero-order shock-wave location. The order-δ^2 results have a kink at $\eta = 1$ which is caused by the switch from the Taylor series expansion to the integrated solution.

The exact solution for a cone at $M_\infty = 20$ with $\theta_b = 20^\circ$ (ref. 18) is also shown for comparison in figure 10(a) with the case $m = 1.0$. Although the conical bodies are not exactly the same $\left(\theta_b = 20^\circ \text{ corresponds to } \delta = 0.3978\right)$, the nondimensionalized order-δ^2 similarity results agree well with the $M_\infty = 20$ solution shown for all the variables except the density. As can be seen by the symbols representing the exact solution for $M_\infty \to \infty$ at the shock wave, the density is the only one of the flow variables that is affected much by the differences between $M_\infty = 20$ and $M_\infty \to \infty$. The similarity solutions for the density agree exactly with infinite Mach number solution at the shock. The order-δ^2 solution for the other variables differs from the exact, infinite Mach number solution at the shock by amounts which are of order-δ^4, as expected from the approximation to the oblique-shock relations used (eqs. (4)). On the other hand, the zero-order similarity solution is not accurate for a cone of this thickness; it is off by an amount of order-δ^2, which is 16 percent for $\delta = 0.4$.

For body power-law exponents other than $m = 1$ there is no exact solution available for comparison with the order-δ^2 solution. However, there are some simple empirical methods for estimating the pressure on general bodies. Two of these methods will be used for comparisons. One is the Newtonian law $C_p = 2 \sin^2\theta_b$. As discussed by Hayes and Probstein (ref. 5), the Newtonian law corresponds to the limits $\gamma \to 1.0$ and $M_\infty \to \infty$; but, it is widely used for more general hypersonic flows in this or modified form. The other empirical prediction is the tangent-cone method, which takes as the pressure at any point on a body the pressure on the cone having the same surface angle as the body point. This method also is most accurate for $M_\infty \to \infty$, since then the shock layer is very thin with little pressure change across it. Hayes and Probstein (ref. 5) give a thorough discussion of these two methods and their limitations. Only one limitation will be mentioned here: these methods give only the body surface pressure and are not complete flow-field solutions, as are the similarity solutions.

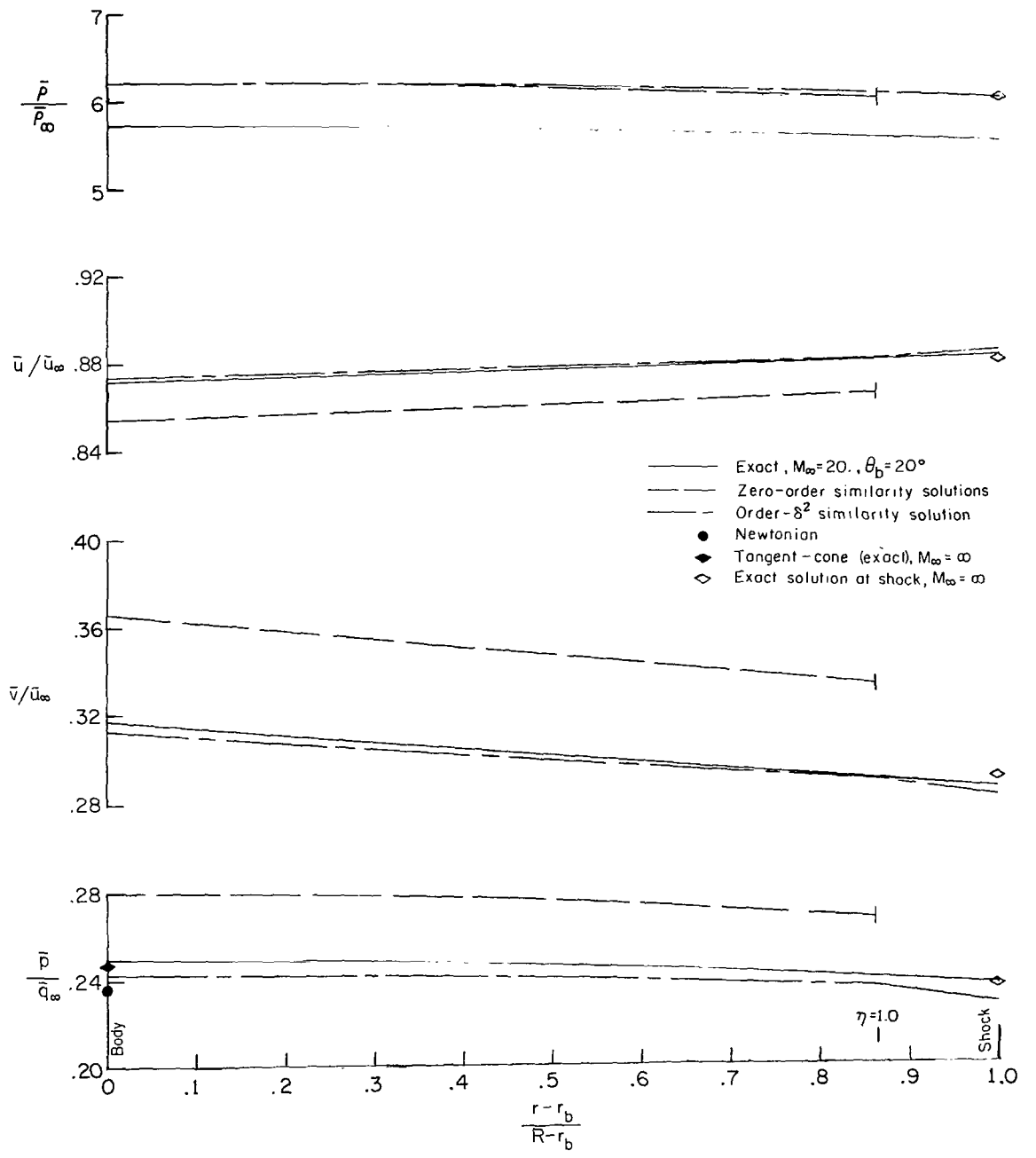

(a) Power-law exponent, m = 1.0 (conical body).

Figure 10.- Variation of flow variables from body to shock at $\bar{x}/\bar{l} = 0.5$ for axisymmetric flow with $\delta = 0.4$.

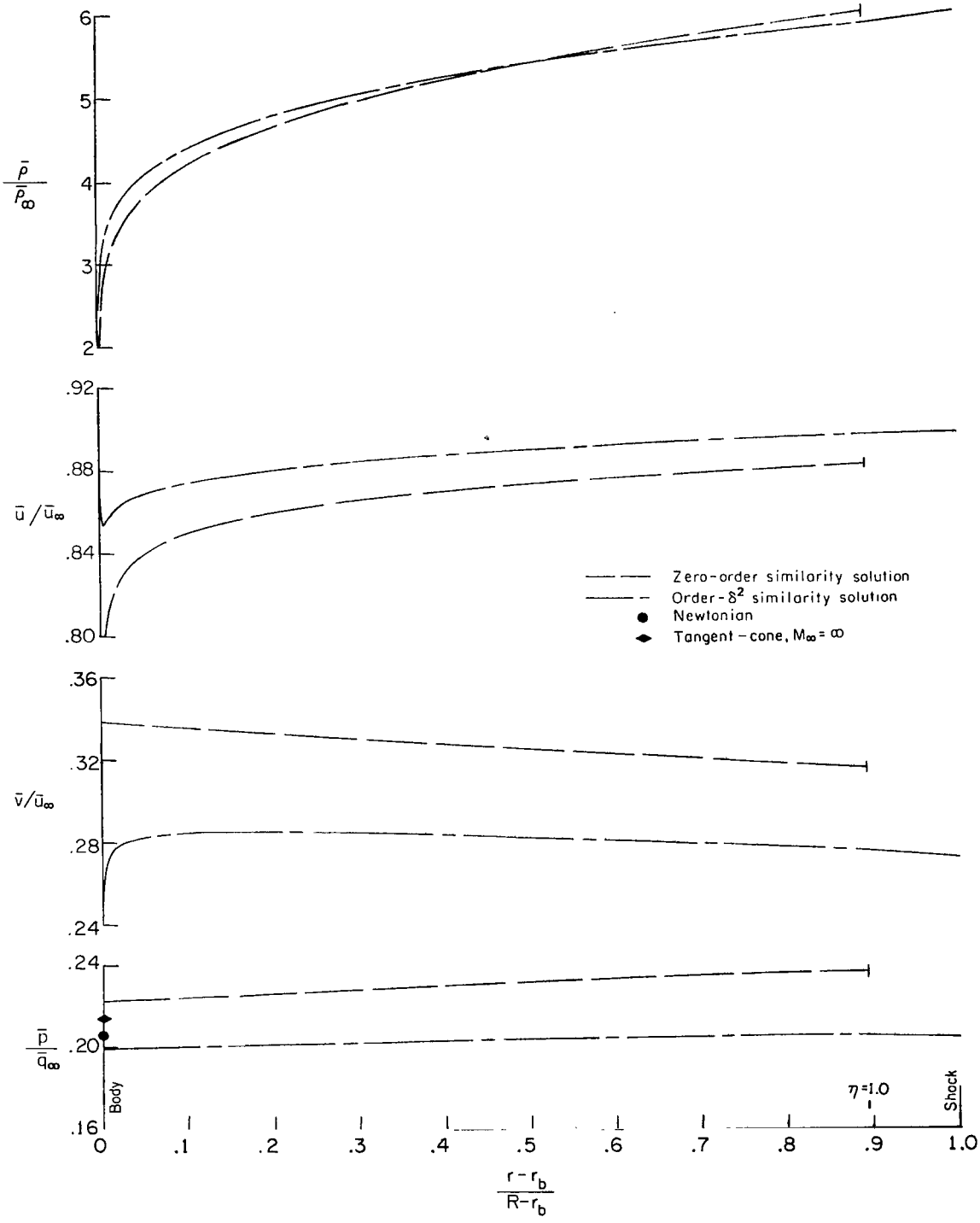

(b) Power-law exponent, m = 0.85.

Figure 10.- Continued.

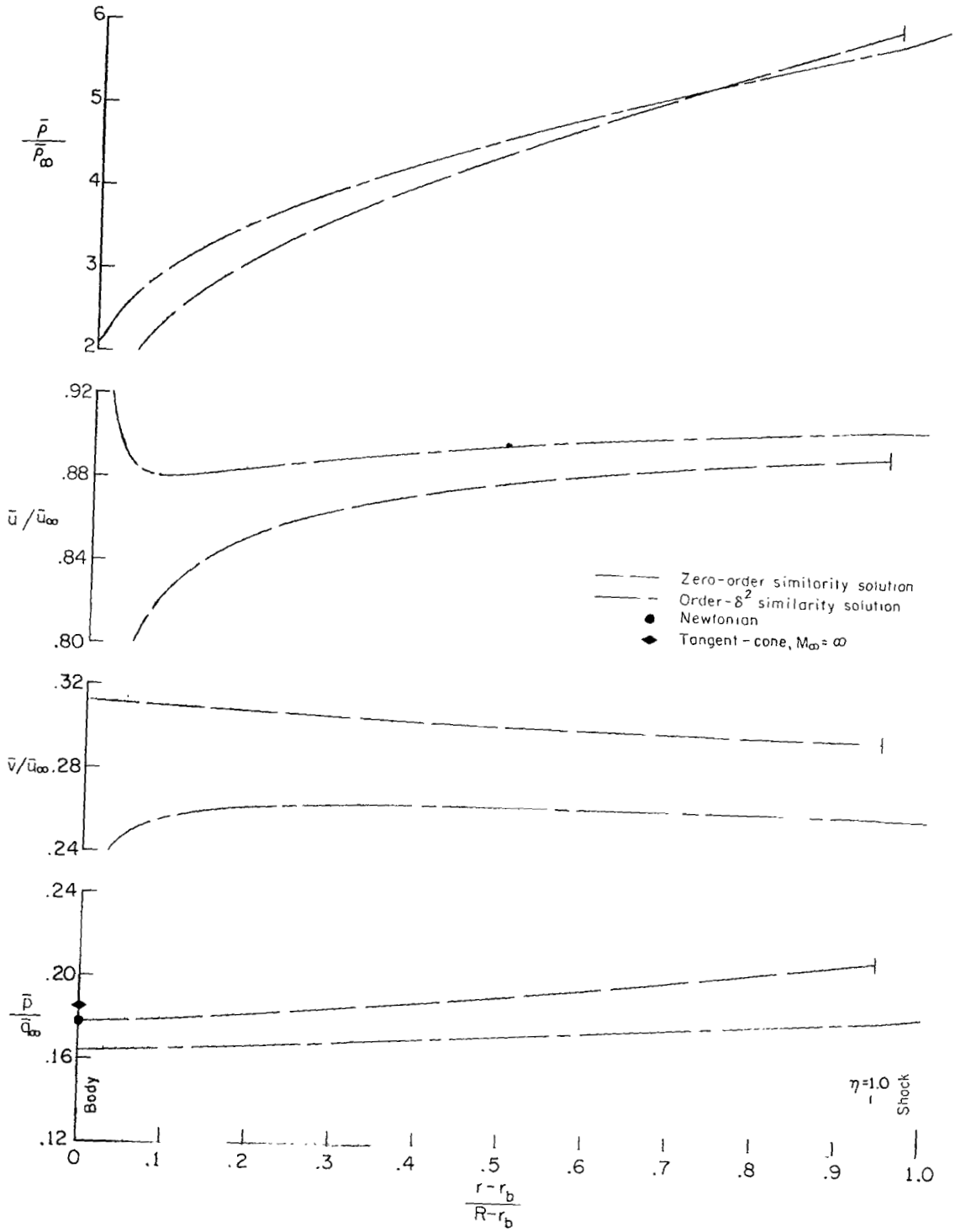

(c) Power-law exponent, m = 0.75.

Figure 10.- Concluded.

The calculated flow fields for bodies having $m = 0.85$ and $m = 0.75$ are shown in figures 10(b) and (c), respectively. In these cases the order-δ^2 solution is again a major correction to the zero-order solution. However, the singularities in some of the order-δ^2 similarity functions show up here at the body surface. Because of the singularities, the order-δ^2 values of the density and the velocity components are probably unrealistic close to the surface. Fortunately, the pressure is well behaved all the way to the body surface, so that surface-pressure coefficients can be calculated.

The surface pressures calculated from the similar solutions are seen in figures 10(a), (b), and (c) to agree fairly well with the empirical predictions of the Newtonian and tangent-cone methods. However, as m goes from 1.0 to 0.85 to 0.75, the order-δ^2 similarity solution pressure drops faster than the tangent-cone and Newtonian pressures, so that the agreement becomes progressively worse. Whether the similarity solution or the empirical methods give a better representation of the actual pressure changes with body power law must be determined by comparison with experiment, as in the following section.

Comparison With Experimental Results

Only a limited amount of useful experimental data exist on the hypersonic flow fields about power-law bodies. These data consist mainly of measured shock-wave shapes and surface-pressure distributions for 3/4- and 2/3-power bodies of a few different fineness ratios. In this section the similarity-solution predictions for shock-wave shape and surface pressure for axisymmetric bodies with power-law exponent of $m = 0.75$ will be compared with the experimental results of Kubota (ref. 3) and Peckham (ref. 7). No comparison is made with results for smaller power-law exponents since valid order-δ^2 similarity solutions were not obtained in those cases. Also, no comparisons are made with experimental total-drag measurements (e.g., those of ref. 10) because of the uncertainty in calculating the skin-friction contribution.

Shock shape.- Because the shock displacement constant a_2 is so small, the order-δ^2 shock-wave shape is only slightly different from the zero-order shape, an example of which is shown in figure 1 ($m = 0.85$; $\sigma = 0$; $\delta = 0.4$). The zero-order and order-δ^2 shock-wave shape predictions are compared to the shock-shape data for $m = 0.75$ from references 3 and 7 in figure 11. These data are presented in the correlation form discussed in the appendix to reference 7. The additional shock-wave-shape data from hypersonic flows over power-law bodies (refs. 8 and 9) are not presented here because they fall in ranges of very large $\bar{x}/\bar{D}$ values, for which the order-δ^2 term of the shock-wave-shape equation is negligible. Also shown in figure 11 is the shock-wave shape, calculated by an asymptotic time-dependent finite-difference method (ref. 19, page 305), for an 0.75-power body having a paraboloidal nose at $M_\infty = \infty$.

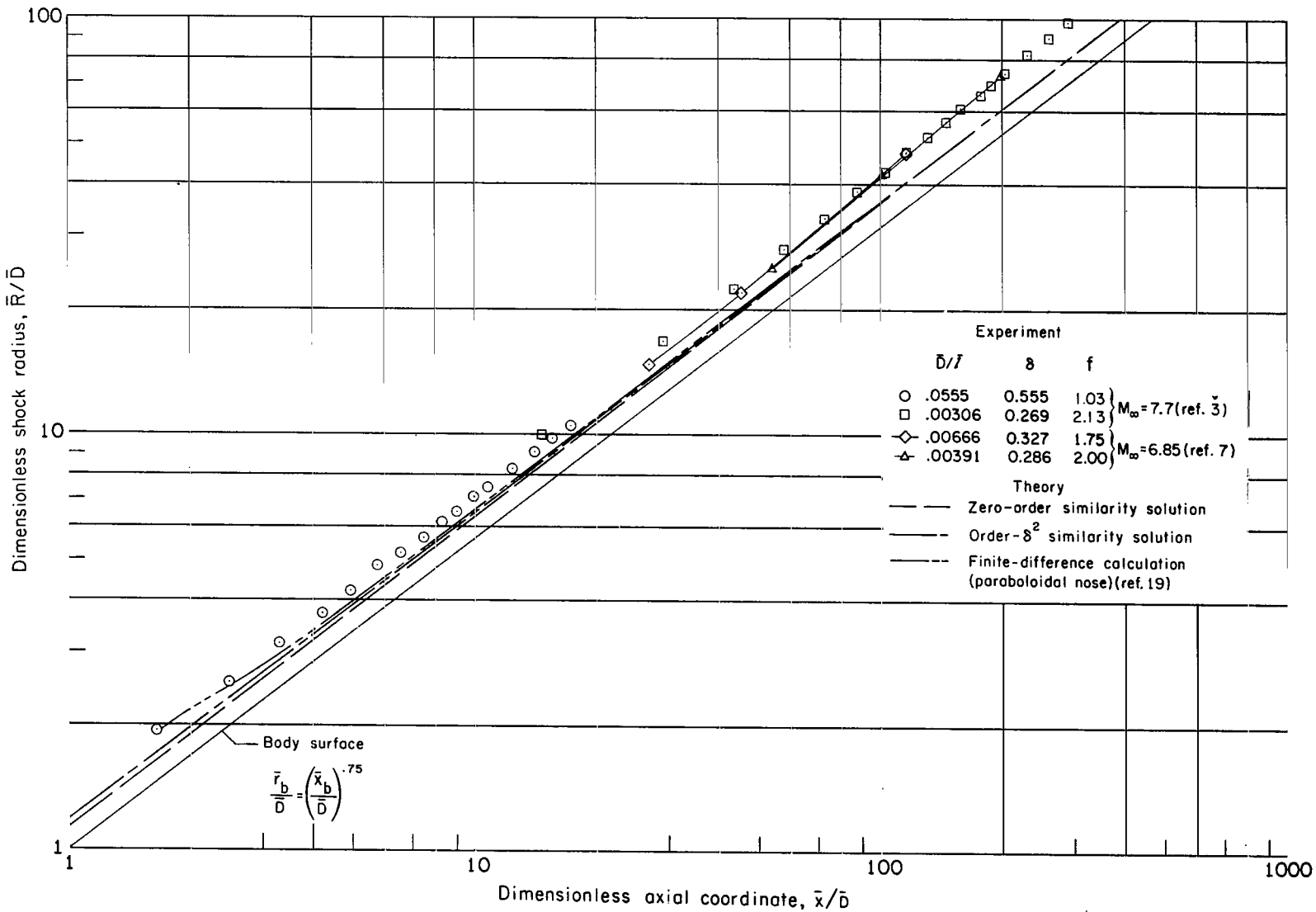

Figure 11.- Shock-wave shape correlation for axisymmetric 3/4-power bodies.

The order-δ^2 similarity solution agrees very well with the finite-difference calculation except at small $x/\bar{D}$ values where the latter is affected by its paraboloidal nose shape. The experimental data for the shock shapes are seen to correlate well with one another but to fall somewhat above the similarity solution and finite-difference predictions. This disagreement between experiment and theory is due in part to the disagreement in Mach numbers ($M_\infty = 6.85$ and 7.7 for experiment, $M_\infty = \infty$ for theory). It is comparable to the shift in shock location with Mach number for cones (fig. 9(a)). An additional cause for the disagreement between the experiment and theory is the outward displacement of the flow by the growth of the viscous boundary layer on the experimental bodies.

The effect of the order-δ^2 term in the similarity solution for the shock-wave shape is seen in figure 11 to increase as $\bar{x}/\bar{D}$ decreases. This is expected since small values of $\bar{x}/\bar{D}$ correspond either to small values of $\bar{x}/\bar{l}$ or to large values of $\bar{D}/\bar{l}$, that is, either to points near the nose of the body (where the slope is large) or to bodies which are less slender (and thus have larger δ-values). Note that the agreement of experiment with theory is better in this region of smaller $\bar{x}/\bar{D}$ values, as would be expected since the shock location is closer to that for infinite Mach number for larger body slopes. The slope of the order-δ^2 similarity solution agrees very well with the slope of Kubota's data for $\bar{D}/\bar{l} = 0.0555$ (see circles in fig. 11); this agreement in the slope on a log-log plot indicates good agreement with the power-law exponent of the physical shock-wave shape.

Pressure distribution.- The experimental pressure distributions obtained by Kubota (ref. 3) and Peckham (ref. 7) are shown in figure 12 for the same power-law bodies ($m = 0.75$) as used for the shock-wave shapes. For comparison, the zero-order and order-δ^2 similarity-solution predictions are also shown, along with the two empirical pressure distributions. For the three bodies having fineness ratios $f \equiv \bar{l}/2r_b(\bar{l})$ of about 2, the similarity solutions, as well as the two empirical methods, give pressure distributions in good agreement with the experimental data.

For these cases the order-δ^2 similarity solution is very nearly the same as the zero-order solution except at the front of the body. The Newtonian prediction falls slightly higher than the similarity solutions behind the nose region, but curves representing these three methods are below the data points. Since at hypersonic speeds the viscous boundary layer tends to displace the flow outward, raising the pressure above that which would occur for inviscid flow, the theoretical inviscid pressure levels are expected to fall slightly below those actually measured. For example, by applying a boundary-layer displacement correction to the zero-order similarity solution for the pressure on his fineness-ratio-2.13 body, Kubota (ref. 3) obtained excellent agreement with his experimental data. (See squares in fig. 12.) Since the tangent-cone pressure

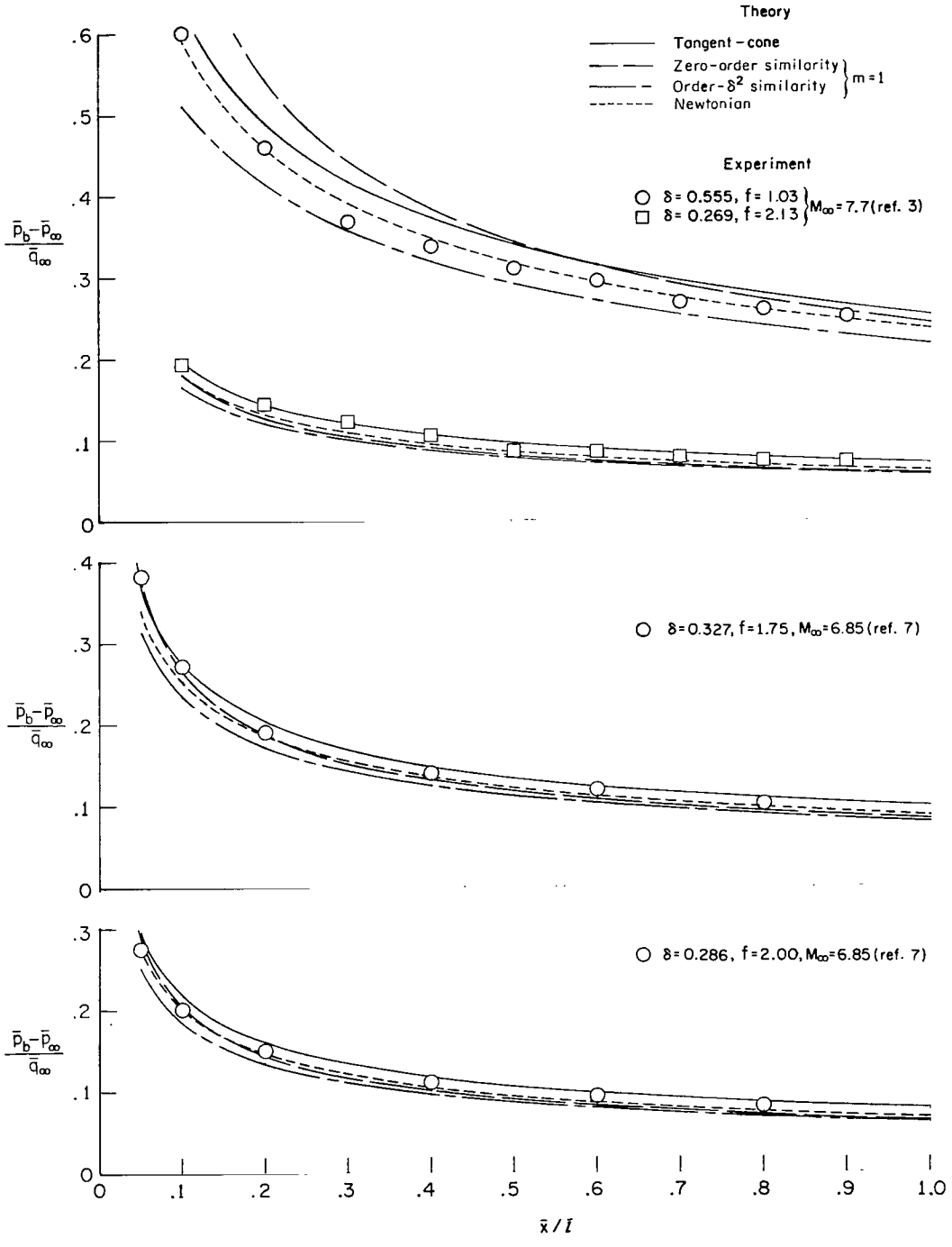

Figure 12.- Comparison of similarity solutions with experimental pressure distributions m = 0.75; theory is for same values of δ as experiment; tangent-cone for same Mach number.

distribution falls slightly above the experimental data for the three higher fineness-ratio bodies, the other methods are somewhat preferable.

Only in the case of the body having a fineness ratio of nearly 1, however, does a real difference between the methods appear in figure 12. In particular, the difference between the zero-order and order-δ^2 pressure distributions becomes substantial. The zero-order result lies above the experimental data by an amount which increases rapidly toward the front of the body. On the other hand, the order-δ^2 result lies below the data by an amount which, for most of the body, is only moderately larger than that for the finer bodies. This amount is on the order of the expected boundary-layer displacement effect. It is only at the front of the body that the order-δ^2 result begins to diverge markedly from the experimental pressure distribution. Since the value of the slenderness parameter is $\delta = 0.555$ for this case, it is not surprising that the order-δ^2 similarity solution should begin to fail as the body surface angle increases at the front of the body. (Kubota's value $\delta = 0.485$ shown with his data corresponds to $\delta\eta_b = 0.485$ as used herein.) This is about the same value of δ as the limit for good results in the wedge and cone cases (figs. 8 and 9). The Newtonian method gives excellent agreement with the experimental data in this case, but this must be somewhat fortuitous in that no correction was made to account for the boundary-layer displacement or body-curvature effects. The tangent-cone method again lies somewhat above the experimental data.

CONCLUSIONS

By beginning with the equations for conservation of mass, conservation of momentum, and conservation of energy for the inviscid, two-dimensional or axisymmetric adiabatic flow of an ideal gas, similarity solutions have been found which give the flow field to order-δ^2 about power-law bodies in the hypersonic limit $M_\infty \to \infty$, where δ is a body slenderness parameter and M_∞ is the free-stream Mach number. On the basis of this investigation the following conclusions can be made:

1. Order-δ^2 solutions were obtained which are independent of the slenderness parameter δ. Thus, the functions expressing the solutions are universal in that they apply for all values of δ for which $\delta^4 \ll 1$. The relations between those similarity functions and the physical flow variables are relatively simple.

2. In the present formulations the value of a_2, the shock displacement constant in the order-δ^2 solution, goes through plus and minus infinity at about $m = 0.817$ in the two-dimensional case and about $m = 0.653$ in the axisymmetric case, where m is the body power-law exponent. Because the singularity does not correspond to actual flow conditions, it must arise through the mathematical development. Since the singularity was not removed by any of the variations in solution procedure tried, the present results

are limited to a range judged relatively free of effects from the singularity ($0.85 \leqq m \leqq 1.0$ for two-dimensional flow; $0.75 \leqq m \leqq 1.0$ for axisymmetric flow).

3. In comparisons with the exact solutions for inviscid flow over wedges and circular cones, the order-δ^2 similarity results give excellent agreement for δ less than about 0.4, corresponding to wedge or cone angles up to about 20°. Over an even larger range, the order-δ^2 surface-pressure predictions were superior to the Newtonian pressure law. The order-δ^2 results were a significant improvement over the zero-order results for body angles greater than about 12°.

4. In comparisons with experimental shock-wave shapes and surface-pressure distributions for 3/4-power axisymmetric bodies, the order-δ^2 similarity solutions gave good results, considering that Mach number and boundary-layer displacement effects are not included in the theory. For body fineness ratios near 2, the effects of the order-δ^2 terms are significant only very near the body nose; whereas for a fineness ratio near 1, the order-δ^2 terms had a large effect over almost the entire body. These good results for the surface pressure were obtained despite the singular behavior of some other variables at the surface.

5. Although the order-δ^2 similarity solutions were developed for the hypersonic limit $M_\infty \to \infty$, the derivation shows that they are compatible with order-ϵ solutions, where $\epsilon \equiv 1/(M_\infty \delta)^2$, which introduce Mach number effects.

Langley Research Center
National Aeronautics and Space Administration
Hampton, Va. 23665
July 1, 1975

APPENDIX

APPLICATION OF THE ORDER-δ^2 SOLUTIONS

In order to facilitate application of the order-δ^2 similarity solutions, the equations relating the similarity functions to the physical-flow variables are presented here. It is assumed that the body fineness ratio f and power-law exponent m are known, so that the body shape is

$$\frac{\bar{r}_b}{\bar{l}} = \frac{1}{2f}\left(\frac{\bar{x}}{\bar{l}}\right)^m$$

The value of σ is 0 for a two-dimensional body and is 1 for an axisymmetric body. Then, the values of η_b, the body-surface similarity coordinate, and of a_2, the shock displacement constant, are found in table III for the given m. The value of δ, the slenderness parameter, is calculated from

$$\delta = \frac{1}{2f\eta_b}$$

The order-δ^2 shock-wave shape is

$$\frac{\bar{R}}{\bar{l}} = \delta\left(\frac{\bar{x}}{\bar{l}}\right)^m\left[1 + \delta^2 a_2 m^2\left(\frac{\bar{x}}{\bar{l}}\right)^{-2(1-m)}\right]$$

The similarity coordinates of any point $(\bar{x},\bar{r})$ in the flow field between the body and the shock wave are

$$\xi = \frac{\bar{x}}{\bar{l}} \qquad \eta = \eta_b\left(\frac{\bar{r}}{\bar{r}_b}\right)$$

By taking the values of the similarity functions from table I (for two-dimensional flow) or table II (for axisymmetric flow), the pressure, density, and velocity components at any point (ξ,η) are given to order-δ^2 by

$$\frac{\bar{p}}{\bar{q}_\infty} = 2\delta^2\left[F_0(\eta)m^2\xi^{-2(1-m)} + \delta^2 F_2(\eta)m^4\xi^{-4(1-m)}\right]$$

APPENDIX

$$\frac{\bar{\rho}}{\bar{\rho}_\infty} = \psi_0(\eta) + \delta^2\psi_2(\eta)m^2\xi^{-2(1-m)}$$

$$\frac{\bar{u}}{\bar{u}_\infty} = 1 + \delta^2\nu_0(\eta)m^2\xi^{-2(1-m)}$$

$$\frac{\bar{v}}{\bar{u}_\infty} = \delta\phi_0(\eta)m\xi^{-(1-m)} + \delta^3\phi_2(\eta)m^3\xi^{-3(1-m)}$$

Because the entropy layer makes the similarity solutions for the velocity and density inapplicable at the body surface for $m < 1$, these flow variables must be found by other means. The similarity solution for the pressure, on the other hand, does give a reasonable result at the surface, which can be used to help in calculating the density and velocity. The basis of the method for calculating the density and velocity at the surface is the fact that the streamline along the surface must have passed through the normal shock wave at the blunt nose of the body. After passing through the shock, the flow is isentropic along streamlines. Thus, by letting the subscript n denote conditions just behind the normal shock, and by using isentropic and normal shock relations (e.g., ref. 14), the density at the surface is

$$\frac{\bar{\rho}_b}{\bar{\rho}_\infty} = \frac{\bar{\rho}_n}{\bar{\rho}_\infty}\frac{\bar{\rho}_b}{\bar{\rho}_n} = \frac{\bar{\rho}_n}{\bar{\rho}_\infty}\left(\frac{\bar{p}_b}{\bar{p}_n}\right)^{1/\gamma}$$

$$= \frac{\bar{\rho}_n}{\bar{\rho}_\infty}\left[\gamma\delta^2 M_\infty{}^2 p\left(\xi,\eta_b\right)\Big/\left(\frac{\bar{p}_n}{\bar{p}_\infty}\right)\right]^{1/\gamma}$$

$$= \left[\frac{(\gamma+1)M_\infty{}^2}{(\gamma-1)M_\infty{}^2+2}\right]\left[\frac{\gamma(\gamma+1)M_\infty{}^2}{2\gamma M_\infty{}^2-(\gamma-1)}\,\delta^2 p\left(\xi,\eta_b\right)\right]^{1/\gamma}$$

Similarly, the magnitude of the velocity at the surface is given by

APPENDIX

$$\bar{V}_b^{\,2} = \frac{2\gamma}{\gamma - 1}\left[\left(\frac{p_t}{\rho_t}\right)_\infty - \frac{\bar{p}_b}{\bar{\rho}_b}\right]$$

$$= \frac{2\gamma}{\gamma - 1}\frac{\bar{p}_\infty}{\bar{\rho}_\infty}\left[\frac{T_t}{T_\infty} - \left(\frac{\bar{p}_b/\bar{p}_\infty}{\bar{\rho}_b/\bar{\rho}_\infty}\right)\right]$$

or

$$\frac{\bar{V}_b}{\bar{u}_\infty} = \left\{1 + \frac{2}{\gamma - 1}\left[\frac{1}{M_\infty^{\,2}} - \delta^2\frac{p(\xi,\eta_b)}{\rho(\xi,\eta_b)}\right]\right\}^{1/2}$$

$$= \left\{\left[1 + \frac{2\gamma}{(\gamma - 1)M_\infty^{\,2}}\right]\left[1 - \gamma\left(\frac{2}{\gamma + 1}\right)^{\frac{\gamma+1}{\gamma}}\left(1 - \frac{\gamma - 1}{\gamma M_\infty^{\,2}}\right)^{1/\gamma}\left(\delta^2 p_b\right)^{\frac{\gamma-1}{\gamma}}\right]\right\}^{1/2}$$

In the limit as $M_\infty \to \infty$, the density and velocity become

$$\frac{\bar{\rho}_b}{\bar{\rho}_\infty} = \left(\frac{\gamma + 1}{\gamma - 1}\right)\left(\frac{\gamma + 1}{2}\,\delta^2 p_b\right)^{1/\gamma}$$

and

$$\frac{\bar{V}_b}{\bar{u}_\infty} = \left[1 - \gamma\left(\frac{2}{\gamma + 1}\right)^{\frac{\gamma+1}{\gamma}}\left(\delta^2 p_b\right)^{\frac{\gamma-1}{\gamma}}\right]^{1/2}$$

Here $p_b \equiv \dfrac{p(\bar{x},\bar{r}_b)}{\delta^2\bar{\rho}_\infty\bar{u}_\infty^{\,2}}$ is the normalized surface pressure given by the similarity solutions.

Since the flow at the body is parallel to the surface, the velocity components are

$$\frac{\bar{u}_b}{\bar{u}_\infty} = \frac{\overline{V}_b}{\bar{u}_\infty} \cos \theta_b = \frac{\overline{V}_b}{\bar{u}_\infty} \frac{(\bar{x}/\bar{l})^{1-m}}{\sqrt{(\bar{x}/\bar{l})^{2(1-m)} + \delta^2 \eta_b{}^2 m^2}}$$

and

$$\frac{\bar{v}_b}{\bar{u}_\infty} = \frac{\overline{V}_b}{\bar{u}_\infty} \sin \theta_b = \frac{\overline{V}_b}{\bar{u}_\infty} \frac{\delta \eta_b m}{\sqrt{(\bar{x}/\bar{l})^{2(1-m)} + \delta^2 \eta_b{}^2 m^2}}$$

REFERENCES

1. Lees, Lester: Inviscid Hypersonic Flow Over Blunt-Nosed Slender Bodies. GALCIT Hypersonic Res. Proj. Mem. No. 31 (Contract No. DA-04-495-Ord-19), Feb. 1, 1956.

2. Lees, Lester; and Kubota, Toshi: Inviscid Hypersonic Flow Over Blunt-Nosed Slender Bodies. J. Aeron. Sci., vol. 24, no. 3, Mar. 1957, pp. 195-202.

3. Kubota, Toshi: Investigation of Flow Around Simple Bodies in Hypersonic Flow. GALCIT Memo. No. 40 (Contract No. DA-04-495-Ord-19), June 25, 1957.

4. Mirels, Harold: Approximate Analytical Solutions for Hypersonic Flow Over Slender Power Law Bodies. NASA TR R-15, 1959.

5. Hayes, Wallace D.; and Probstein, Ronald F.: Hypersonic Flow Theory. Volume I – Inviscid Flows. Second ed., Academic Press, Inc., 1966.

6. Mirels, Harold: Hypersonic Flow Over Slender Bodies Associated With Power-Law Shocks. Vol. 7 of Advances in Applied Mechanics, H. L. Dryden and Th. von Kármán, eds., Academic Press, Inc., 1962, pp. 1-54.

7. Peckham, D. H.: Measurements of Pressure Distribution and Shock-Wave Shape on Power-Law Bodies at a Mach Number of 6.85. C.P. No. 871, British A.R.C., 1967. (Replaces R.A.E. Tech. Rep. No. 65075.)

8. Freeman, N. C.; Cash, R. F.; and Bedder, D.: An Experimental Investigation of Asymptotic Hypersonic Flows. J. Fluid Mech., vol. 18, pt. 3, Mar. 1964, pp. 379-384.

9. Beavers, G. S.: Shock-Wave Shapes on Hypersonic Axisymmetric Power-Law Bodies. AIAA J., vol. 7, no. 10, Oct. 1969, pp. 2038-2040.

10. Spencer, Bernard, Jr.; and Fox, Charles H., Jr.: Hypersonic Aerodynamic Performance of Minimum-Wave-Drag Bodies. NASA TR R-250, 1966.

11. Ashby, George C., Jr.: Longitudinal Aerodynamic Performance of a Series of Power-Law and Minimum-Wave-Drag Bodies at Mach 6 and Several Reynolds Numbers. NASA TM X-2713, 1974.

12. Ashby, George C., Jr.; and Harris, Julius E.: Boundary-Layer Transition and Displacement-Thickness Effects on Zero-Lift Drag of a Series of Power-Law Bodies at Mach 6. NASA TN D-7723, 1974.

13. Townsend, James C.: Hypersonic Aerodynamic Characteristics of a Family of Power-Law, Wing-Body Configurations. NASA TN D-7427, 1973.

14. Townsend, James C.: Second-Order Small Disturbance Theory for Hypersonic Flow Over Power-Law Bodies. Ph. D. Diss., Univ. of Virginia, 1974.

15. Equations, Tables, and Charts for Compressible Flow. NACA Rep. 1135, 1953.

16. Van Dyke, Milton: Perturbation Methods in Fluid Mechanics. Academic Press, Inc., 1964.

17. Freeman, N. C.: Asymptotic Solutions in Hypersonic Flow: An Approach to Second-Order Solutions of Hypersonic Small-Disturbance Theory. Research Frontiers in Fluid Dynamics, Raymond J. Seeger and G. Temple, eds., Interscience Publ., c.1965, pp. 284-307.

18. Sims, Joseph L.: Tables for Supersonic Flow Around Right Circular Cones at Zero Angle of Attack. NASA SP-3004, 1964.

19. Lyubimov, A. N.; and Rusanov, V. V.: Gas Flows Past Blunt Bodies. Part I: Calculation Method and Flow Analysis. NASA TT F-714, 1973.

TABLE I.- SIMILARITY FUNCTIONS FOR TWO-DIMENSIONAL FLOW ($\sigma = 0$)

η	F_0	ψ_0	ν_0	ϕ_0	F_2	ψ_2	ν_2	ϕ_2
				m = 1.00				
1.00000	.83333	6.0000	.83333	.83333	-.5556	0.0000	-.5556	-.6944
.99219	.83333	6.0000	.83333	.83333	-.5556	0.0000	-.5556	-.6944
.98438	.83333	6.0000	.83333	.83333	-.5556	0.0000	-.5556	-.6944
.97656	.83333	6.0000	.83333	.83333	-.5556	0.0000	-.5556	-.6944
.96875	.83333	6.0000	.83333	.83333	-.5556	0.0000	-.5556	-.6944
.96094	.83333	6.0000	.83333	.83333	-.5556	0.0000	-.5556	-.6944
.95313	.83333	6.0000	.83333	.83333	-.5556	0.0000	-.5556	-.6944
.94531	.83333	6.0000	.83333	.83333	-.5556	0.0000	-.5556	-.6944
.93750	.83333	6.0000	.83333	.83333	-.5556	0.0000	-.5556	-.6944
.92969	.83333	6.0000	.83333	.83333	-.5556	0.0000	-.5556	-.6944
.92188	.83333	6.0000	.83333	.83333	-.5556	0.0000	-.5556	-.6944
.91406	.83333	6.0000	.83333	.83333	-.5556	0.0000	-.5556	-.6944
.90625	.83333	6.0000	.83333	.83333	-.5556	0.0000	-.5556	-.6944
.89844	.83333	6.0000	.83333	.83333	-.5556	0.0000	-.5556	-.6944
.89063	.83333	6.0000	.83333	.83333	-.5556	0.0000	-.5556	-.6944
.88281	.83333	6.0000	.83333	.83333	-.5556	0.0000	-.5556	-.6944
.87500	.83333	6.0000	.83333	.83333	-.5556	0.0000	-.5556	-.6944
.86719	.83333	6.0000	.83333	.83333	-.5556	0.0000	-.5556	-.6944
.85938	.83333	6.0000	.83333	.83333	-.5556	0.0000	-.5556	-.6944
.85156	.83333	6.0000	.83333	.83333	-.5556	0.0000	-.5556	-.6944
.84375	.83333	6.0000	.83333	.83333	-.5556	0.0000	-.5556	-.6944
.83594	.83333	6.0000	.83333	.83333	-.5556	0.0000	-.5556	-.6944
.83333	.83333	6.0000	.83333	.83333	-.5556	0.0000	-.5556	-.6944
				m = 0.95				
1.00000	.83333	6.0000	.83333	.83333	-.6414	-.8290	-.6107	-.7259
.99219	.83030	5.9629	.83373	.83232	-.6307	-.7645	-.6086	-.7232
.98438	.82735	5.9254	.83425	.83133	-.6205	-.7018	-.6068	-.7207
.97656	.82448	5.8876	.83489	.83038	-.6107	-.6409	-.6054	-.7185
.96875	.82170	5.8493	.83566	.82944	-.6014	-.5813	-.6042	-.7165
.96094	.81899	5.8103	.83658	.82854	-.5924	-.5231	-.6034	-.7148
.95313	.81636	5.7706	.83764	.82765	-.5839	-.4658	-.6029	-.7132
.94531	.81380	5.7300	.83887	.82679	-.5757	-.4094	-.6028	-.7119
.93750	.81131	5.6884	.84029	.82595	-.5678	-.3536	-.6031	-.7109
.92969	.80888	5.6454	.84191	.82513	-.5602	-.2982	-.6038	-.7101
.92188	.80652	5.6010	.84375	.82434	-.5529	-.2430	-.6049	-.7095
.91406	.80422	5.5548	.84586	.82356	-.5460	-.1875	-.6065	-.7093
.90625	.80199	5.5064	.84826	.82280	-.5392	-.1316	-.6087	-.7094
.89844	.79981	5.4554	.85101	.82205	-.5328	-.0749	-.6115	-.7098
.89063	.79769	5.4013	.85418	.82133	-.5266	-.0167	-.6151	-.7106
.88281	.79562	5.3433	.85786	.82062	-.5206	.0434	-.6196	-.7119
.87500	.79361	5.2805	.86216	.81993	-.5148	.1062	-.6251	-.7138
.86719	.79166	5.2113	.86727	.81925	-.5093	.1730	-.6322	-.7164
.85938	.78977	5.1338	.87346	.81858	-.5039	.2453	-.6411	-.7199
.85156	.78793	5.0448	.88116	.81793	-.4988	.3257	-.6528	-.7247
.84375	.78616	4.9387	.89113	.81730	-.4939	.4185	-.6686	-.7314
.83594	.78445	4.8049	.90489	.81668	-.4892	.5324	-.6916	-.7412
.82813	.78282	4.6180	.92629	.81607	-.4847	.6879	-.7293	-.7573
.82031	.78130	4.2817	.97116	.81547	-.4805	.9657	-.8157	-.7925
.81507	.78040			.81507	-.4780			

TABLE I.- Concluded

η	F_0	ψ_0	ν_0	ϕ_0	F_2	ψ_2	ν_2	ϕ_2
				m = 0.90				
1.00000	.83333	6.0000	.83333	.83333	-.7518	-1.7618	-.6865	-.7681
.99219	.82693	5.9221	.83417	.83119	-.7281	-1.6059	-.6836	-.7624
.98438	.82075	5.8444	.83523	.82910	-.7057	-1.4558	-.6814	-.7572
.97656	.81478	5.7668	.83652	.82707	-.6844	-1.3112	-.6799	-.7525
.96875	.80900	5.6893	.83807	.82508	-.6642	-1.1716	-.6792	-.7481
.96094	.80342	5.6115	.83989	.82315	-.6449	-1.0365	-.6793	-.7442
.95313	.79802	5.5335	.84200	.82126	-.6266	-.9056	-.6802	-.7408
.94531	.79281	5.4548	.84441	.81941	-.6091	-.7783	-.6820	-.7378
.93750	.78776	5.3755	.84716	.81761	-.5926	-.6543	-.6846	-.7352
.92969	.78288	5.2952	.85028	.81585	-.5767	-.5331	-.6883	-.7331
.92188	.77816	5.2137	.85380	.81414	-.5617	-.4143	-.6931	-.7315
.91406	.77360	5.1307	.85777	.81246	-.5473	-.2974	-.6991	-.7304
.90625	.76919	5.0456	.86225	.81081	-.5337	-.1820	-.7064	-.7299
.89844	.76493	4.9588	.86731	.80921	-.5206	-.0675	-.7153	-.7300
.89063	.76082	4.8691	.87303	.80764	-.5082	.0466	-.7260	-.7307
.88281	.75685	4.7761	.87953	.80610	-.4964	.1612	-.7388	-.7322
.87500	.75302	4.6792	.88693	.80459	-.4851	.2768	-.7541	-.7345
.86719	.74933	4.5776	.89543	.80311	-.4744	.3946	-.7725	-.7377
.85938	.74578	4.4700	.90527	.80167	-.4641	.5157	-.7948	-.7422
.85156	.74237	4.3551	.91681	.80025	-.4544	.6418	-.8220	-.7481
.84375	.73910	4.2308	.93053	.79886	-.4452	.7750	-.8559	-.7558
.83594	.73598	4.0941	.94718	.79749	-.4365	.9184	-.8991	-.7658
.82813	.73301	3.9406	.96798	.79615	-.4282	1.0769	-.9560	-.7793
.82031	.73020	3.7631	.99502	.79483	-.4205	1.2587	-1.0347	-.7977
.81250	.72757	3.5483	1.03251	.79353	-.4133	1.4788	-1.1526	-.8244
.80469	.72515	3.2672	1.09065	.79226	-.4066	1.7720	-1.3558	-.8674
.79688	.72301	2.8296	1.20714	.79100	-.4007	2.2552	-1.8408	-.9565
.78988	.72154			.78988	-.3966			
				m = 0.85				
1.00000	.83333	6.0000	.83333	.83333	-.8590	-1.6653	-.7974	-.8231
.99219	.82320	5.8770	.83464	.82993	-.8221	-1.3962	-.7965	-.8145
.98438	.81345	5.7559	.83627	.82660	-.7872	-1.1400	-.7968	-.8066
.97656	.80409	5.6367	.83823	.82334	-.7544	-.8955	-.7984	-.7992
.96875	.79509	5.5190	.84055	.82016	-.7234	-.6620	-.8014	-.7925
.96094	.78644	5.4028	.84325	.81704	-.6942	-.4386	-.8058	-.7863
.95313	.77813	5.2879	.84634	.81400	-.6667	-.2244	-.8117	-.7808
.94531	.77014	5.1739	.84986	.81102	-.6407	-.0187	-.8192	-.7758
.93750	.76246	5.0609	.85383	.80811	-.6162	.1793	-.8285	-.7715
.92969	.75509	4.9484	.85829	.80526	-.5932	.3703	-.8397	-.7678
.92188	.74800	4.8364	.86328	.80247	-.5714	.5552	-.8530	-.7647
.91406	.74119	4.7247	.86886	.79974	-.5509	.7345	-.8686	-.7623
.90625	.73466	4.6128	.87507	.79706	-.5316	.9092	-.8867	-.7606
.89844	.72838	4.5007	.88199	.79444	-.5134	1.0799	-.9078	-.7597
.89063	.72237	4.3880	.88970	.79187	-.4963	1.2473	-.9322	-.7595
.88281	.71660	4.2745	.89829	.78935	-.4801	1.4124	-.9605	-.7603
.87500	.71107	4.1596	.90789	.78687	-.4650	1.5759	-.9932	-.7619
.86719	.70577	4.0432	.91864	.78445	-.4507	1.7389	-1.0311	-.7645
.85938	.70071	3.9246	.93071	.78207	-.4373	1.9023	-1.0754	-.7684
.85156	.69588	3.8034	.94435	.77973	-.4248	2.0674	-1.1274	-.7735
.84375	.69127	3.6789	.95984	.77743	-.4131	2.2355	-1.1889	-.7802
.83594	.68688	3.5504	.97757	.77517	-.4021	2.4085	-1.2624	-.7886
.82813	.68271	3.4168	.99805	.77295	-.3919	2.5885	-1.3514	-.7993
.82031	.67877	3.2770	1.02200	.77076	-.3825	2.7781	-1.4610	-.8126
.81250	.67504	3.1292	1.05040	.76861	-.3737	2.9812	-1.5988	-.8294
.80469	.67155	2.9714	1.08478	.76649	-.3658	3.2029	-1.7770	-.8507
.79688	.66829	2.8002	1.12745	.76440	-.3585	3.4510	-2.0159	-.8783
.78906	.66527	2.6110	1.18236	.76233	-.3520	3.7377	-2.3529	-.9151
.78125	.66252	2.3959	1.25684	.76029	-.3463	4.0845	-2.8652	-.9666
.77344	.66006	2.1407	1.36668	.75827	-.3416	4.5347	-3.7427	-1.0446
.76563	.65794	1.8131	1.55607	.75628	-.3379	5.1985	-5.6225	-1.1824
.75781	.65627	1.3010	2.04995	.75429	-.3358	6.5593	-13.0166	-1.5489
.75311	.65566			.75311	-.3364			

TABLE II.- SIMILARITY FUNCTIONS FOR AXISYMMETRIC FLOW ($\sigma = 1$)

η	F_0	ψ_0	ν_0	ϕ_0	F_2	ψ_2	ν_2	ϕ_2
				m = 1.00				
1.00000	.83333	6.0000	.83333	.83333	-.6091	.4248	-.6091	-.6799
.99219	.84055	6.0371	.84085	.84088	-.6306	.3445	-.6250	-.6959
.98438	.84705	6.0704	.84823	.84835	-.6495	.2746	-.6401	-.7112
.97656	.85284	6.1000	.85550	.85576	-.6660	.2142	-.6546	-.7259
.96875	.85796	6.1261	.86269	.86315	-.6804	.1622	-.6685	-.7402
.96094	.86240	6.1487	.86981	.87053	-.6927	.1180	-.6820	-.7542
.95313	.86617	6.1679	.87689	.87793	-.7030	.0812	-.6951	-.7679
.94531	.86927	6.1837	.88394	.88536	-.7115	.0513	-.7080	-.7814
.93750	.87169	6.1960	.89098	.89284	-.7180	.0283	-.7206	-.7949
.92969	.87342	6.2048	.89804	.90040	-.7226	.0120	-.7332	-.8084
.92188	.87445	6.2100	.90512	.90804	-.7254	.0025	-.7457	-.8218
.91494	.87487	6.2131	.91142	.91488	-.7270	-.0032	-.7567	-.8338
				m = 0.95				
1.00000	.83333	6.0000	.83333	.83333	-.6542	.0228	-.6390	-.6959
.99219	.83754	5.9994	.84131	.83988	-.6651	.0013	-.6530	-.7093
.98438	.84113	5.9935	.84939	.84640	-.6742	-.0103	-.6669	-.7224
.97656	.84415	5.9819	.85765	.85292	-.6815	-.0125	-.6808	-.7354
.96875	.84659	5.9640	.86615	.85945	-.6870	-.0054	-.6949	-.7485
.96094	.84846	5.9392	.87500	.86601	-.6911	.0115	-.7095	-.7618
.95313	.84978	5.9060	.88433	.87262	-.6935	.0388	-.7248	-.7755
.94531	.85053	5.8624	.89437	.87929	-.6945	.0781	-.7413	-.7898
.93750	.85073	5.8047	.90549	.88604	-.6941	.1324	-.7597	-.8051
.92969	.85036	5.7255	.91844	.89288	-.6922	.2084	-.7815	-.8222
.92188	.84943	5.6056	.93522	.89983	-.6889	.3232	-.8105	-.8429
.91406	.84796	5.3556	.96541	.90692	-.6843	.5581	-.8658	-.8760
.91034	.84711			.91034	-.6817			
				m = 0.90				
1.00000	.83333	6.0000	.83333	.83333	-.7075	-.4384	-.6750	-.7156
.99219	.83420	5.9581	.84181	.83877	-.7063	-.3849	-.6876	-.7260
.98438	.83462	5.9101	.85064	.84424	-.7040	-.3240	-.7009	-.7366
.97656	.83462	5.8554	.85992	.84974	-.7008	-.2553	-.7151	-.7477
.96875	.83421	5.7931	.86978	.85531	-.6966	-.1783	-.7303	-.7593
.96094	.83338	5.7220	.88036	.86094	-.6914	-.0921	-.7471	-.7716
.95313	.83215	5.6403	.89192	.86666	-.6854	.0050	-.7660	-.7849
.94531	.83051	5.5452	.90479	.87246	-.6786	.1154	-.7877	-.7995
.93750	.82848	5.4321	.91957	.87837	-.6709	.2434	-.8137	-.8159
.92969	.82606	5.2928	.93733	.88440	-.6624	.3970	-.8464	-.8353
.92188	.82328	5.1101	.96043	.89056	-.6532	.5932	-.8918	-.8597
.91406	.82018	4.8352	.99587	.89686	-.6434	.8813	-.9676	-.8956
.90625	.81691	4.1357	1.09932	.90331	-.6334	1.6166	-1.2321	-.9935
.90465	.81630			.90465	-.6315			

TABLE II.- Concluded

η	F_0	ψ_0	ν_0	ϕ_0	F_2	ψ_2	ν_2	ϕ_2
				m = 0.85				
1.00000	.83333	6.0000	.83333	.83333	-.7700	-.9473	-.7188	-.7402
.99219	.83048	5.9124	.84235	.83752	-.7546	-.7969	-.7310	-.7472
.98438	.82742	5.8191	.85198	.84180	-.7392	-.6442	-.7447	-.7551
.97656	.82415	5.7195	.86233	.84617	-.7239	-.4882	-.7603	-.7638
.96875	.82067	5.6125	.87357	.85064	-.7086	-.3278	-.7782	-.7735
.96094	.81698	5.4968	.88590	.85521	-.6934	-.1615	-.7991	-.7845
.95313	.81309	5.3705	.89961	.85991	-.6782	.0128	-.8236	-.7969
.94531	.80901	5.2312	.91515	.86472	-.6630	.1980	-.8531	-.8112
.93750	.80474	5.0746	.93319	.86967	-.6478	.3984	-.8896	-.8281
.92969	.80030	4.8944	.95489	.87476	-.6326	.6214	-.9367	-.8485
.92188	.79572	4.6790	.98241	.87999	-.6176	.8802	-1.0014	-.8745
.91406	.79105	4.4035	1.02070	.88539	-.6027	1.2035	-1.1007	-.9105
.90625	.78640	3.9979	1.08536	.89095	-.5883	1.6771	-1.2928	-.9706
.89844	.78214	2.9087	1.34315	.89668	-.5754	3.0601	-2.3746	-1.2048
.89743	.78174			.89743	-.5742			
				m = 0.80				
1.00000	.83333	6.0000	.83333	.83333	-.8390	-1.4237	-.7712	-.7712
.99219	.82633	5.8617	.84295	.83612	-.8067	-1.1475	-.7842	-.7746
.98438	.81941	5.7196	.85341	.83904	-.7762	-.8785	-.8000	-.7792
.97656	.81256	5.5731	.86487	.84211	-.7472	-.6149	-.8190	-.7852
.96875	.80578	5.4212	.87751	.84533	-.7197	-.3547	-.8419	-.7926
.96094	.79906	5.2627	.89156	.84869	-.6934	-.0957	-.8695	-.8018
.95313	.79239	5.0960	.90735	.85220	-.6683	.1647	-.9029	-.8129
.94531	.78579	4.9192	.92535	.85587	-.6443	.4295	-.9441	-.8264
.93750	.77925	4.7292	.94626	.85970	-.6214	.7030	-.9957	-.8429
.92969	.77279	4.5215	.97114	.86370	-.5996	.9913	-1.0623	-.8632
.92188	.76644	4.2904	1.00183	.86786	-.5788	1.3041	-1.1520	-.8892
.91406	.76023	4.0232	1.04173	.87219	-.5591	1.6582	-1.2812	-.9238
.90625	.75426	3.6971	1.09836	.87671	-.5407	2.0890	-1.4890	-.9736
.89844	.74865	3.2526	1.19402	.88140	-.5240	2.6922	-1.9067	-1.0587
.89063	.74380	2.3985	1.47814	.88628	-.5102	4.0109	-3.6855	-1.3118
.88798	.74265			.88798	-.5073			
				m = 0.75				
1.00000	.83333	6.0000	.83333	.83333	-.8898	-1.4529	-.8253	-.8091
.99219	.82165	5.8050	.84360	.83452	-.8391	-1.0224	-.8405	-.8087
.98438	.81044	5.6103	.85495	.83590	-.7922	-.6147	-.8609	-.8099
.97656	.79967	5.4150	.86755	.83747	-.7487	-.2265	-.8857	-.8129
.96875	.78932	5.2183	.88157	.83923	-.7085	.1456	-.9162	-.8178
.96094	.77937	5.0190	.89729	.84119	-.6711	.5048	-.9536	-.8249
.95313	.76979	4.8161	.91502	.84333	-.6365	.8546	-.9997	-.8342
.94531	.76058	4.6082	.93524	.84566	-.6044	1.1989	-1.0566	-.8463
.93750	.75172	4.3932	.95858	.84817	-.5746	1.5421	-1.1280	-.8617
.92969	.74322	4.1688	.98598	.85088	-.5470	1.8896	-1.2193	-.8811
.92188	.73509	3.9316	1.01886	.85377	-.5217	2.2491	-1.3391	-.9057
.91406	.72735	3.6765	1.05952	.85686	-.4984	2.6315	-1.5030	-.9377
.90625	.72003	3.3956	1.11208	.86013	-.4773	3.0546	-1.7407	-.9805
.89844	.71322	3.0747	1.18477	.86360	-.4586	3.5515	-2.1186	-1.0414
.89063	.70702	2.6846	1.29784	.86726	-.4426	4.1965	-2.8255	-1.1381
.88281	.70168	2.1423	1.52579	.87110	-.4301	5.2307	-4.7293	-1.3359
.87507	.69806			.87507	-.4253			

TABLE III.- SHOCK DISPLACEMENT CONSTANT AND PRESSURE FUNCTIONS AT THE BODY SURFACE

m	η_b	$F_0(\eta_b)$	$F_2(\eta_b)$	a_2
		$\sigma = 0$		
1.00	.83333	.83333	-.55556	.16667
.95	.81507	.78040	-.47804	.17500
.90	.78988	.72154	-.39659	.17618
.85	.75311	.65566	-.33641	.10485
		$\sigma = 1$		
1.00	.91494	.87487	-.72701	.08496
.95	.91034	.84711	-.68169	.08661
.90	.90465	.81630	-.63154	.08768
.85	.89743	.78174	-.57424	.08705
.80	.88798	.74265	-.50734	.08135
.75	.87507	.69806	-.42532	.05812

"The aeronautical and space activities of the United States shall be conducted so as to contribute . . . to the expansion of human knowledge of phenomena in the atmosphere and space. The Administration shall provide for the widest practicable and appropriate dissemination of information concerning its activities and the results thereof."

—NATIONAL AERONAUTICS AND SPACE ACT OF 1958

NASA SCIENTIFIC AND TECHNICAL PUBLICATIONS

TECHNICAL REPORTS: Scientific and technical information considered important, complete, and a lasting contribution to existing knowledge.

TECHNICAL NOTES: Information less broad in scope but nevertheless of importance as a contribution to existing knowledge.

TECHNICAL MEMORANDUMS: Information receiving limited distribution because of preliminary data, security classification, or other reasons. Also includes conference proceedings with either limited or unlimited distribution.

CONTRACTOR REPORTS: Scientific and technical information generated under a NASA contract or grant and considered an important contribution to existing knowledge.

TECHNICAL TRANSLATIONS: Information published in a foreign language considered to merit NASA distribution in English.

SPECIAL PUBLICATIONS: Information derived from or of value to NASA activities. Publications include final reports of major projects, monographs, data compilations, handbooks, sourcebooks, and special bibliographies.

TECHNOLOGY UTILIZATION PUBLICATIONS: Information on technology used by NASA that may be of particular interest in commercial and other non-aerospace applications. Publications include Tech Briefs, Technology Utilization Reports and Technology Surveys.

Details on the availability of these publications may be obtained from:

SCIENTIFIC AND TECHNICAL INFORMATION OFFICE

NATIONAL AERONAUTICS AND SPACE ADMINISTRATION

Washington, D.C. 20546